PCCP

ROYAL SOCIETY OF CHEMISTRY

REVIEW

View Article Online
View Journal | View Issue

Cite this: *Phys. Chem. Chem. Phys.*, 2024, **26**, 11217

Cellulose, cellulose derivatives and cellulose composites in sustainable corrosion protection: challenges and opportunities

Chandrabhan Verma, *[a] Vidusha Singh[b] and Akram AlFantazi*[a]

Received 13th December 2023,
Accepted 19th March 2024

DOI: 10.1039/d3cp06057h

rsc.li/pccp

The use of cellulose-based compounds in coating and aqueous phase corrosion prevention is becoming more popular because they provide excellent protection and satisfy the requirements of green chemistry and sustainable development. Cellulose derivatives, primarily carboxymethyl cellulose (CMC) and hydroxyethyl cellulose (HEC), are widely employed in corrosion prevention. They function as efficient inhibitors by adhering to the metal's surface and creating a corrosion-inhibitive barrier by binding using their –OH groups. Their inhibition efficiency (%IE) depends upon various factors, including their concentration, temperature, chemical composition, the nature of the metal/electrolyte and availability of synergists (X^-, Zn^{2+}, surfactants and polymers). Cellulose derivatives also possess potential applications in anticorrosive coatings as they prevent corrosive species from penetrating and encourage adhesion and cohesion, guaranteeing the metal substrate underneath long-term protection. The current review article outlines the developments made in the past and present to prevent corrosion in both the coating phase and solution by using cellulose derivatives. Together with examining the difficulties of the present and the prospects for the future, the corrosion inhibition mechanism of cellulose derivatives in the solution and coating phases has also been investigated.

1. Introduction

1.1. Fundamentals of cellulose, alkoxycellulose, nanocellulose and cellulose composites

Cellulose (chemical formula; $(C_6H_{10}O_5)_n$) is a polysaccharide, or complex carbohydrate, comprising three thousand or more glucose units. Cellulose is the fundamental structural element of plant cell walls (Fig. 1). Cellulose makes up approximately 33% of all vegetable matter (50% of wood and 90% of cotton). It is the most prevalent naturally occurring organic compound.[1,2] Nondigestible by humans, cellulose is fed to herbivorous animals (like cows and horses) because it is retained in their stomachs for a long enough period to be broken down by microorganisms found in the digestive tract; termites' guts also contain protozoans that break down cellulose. Cellulose is a material of significant economic value processed to create fibers and papers.[3,4] Cellulose undergoes chemical modification to produce materials used in making rayon, plastics, and photographic films, among other products.[5,6] Adhesives, explosives, food thickeners, and moisture-resistant coatings are other products derived from cellulose.[7] A significant structural element of the primary cell wall of oomycetes, various algae, and green plants is cellulose.[8] Specific bacterial species release it to create biofilms. On Earth, cellulose is the most prevalent organic polymer. The primary products made from cellulose are paper and paperboard. A vast range of derivative products, including rayon and cellophane, are produced in smaller quantities. The two primary sources of cellulose used in industry are cotton and wood pulp.[1] Although modified forms of cellulose, or cellulose derivatives, are even more beneficial to the industry, pure cellulose is still a valuable natural product with various biological and industrial uses.

Functionalization of cellulose yields a variety of derivatives (Fig. 2) with possible uses in industry, biology, and the environment.[9–11] Cellulose derivatives are necessary for explosives, films, textiles, and packaging.[12] Thus, it is possible to produce derivatives of solubilized cellulose in both water and alkali.[13] Cellulose derivatives are used in various research analyses as thickening agents for food, ointments, pastes, and creams; they are also used as absorbable surgical agents, sizing agents for paper and textiles, and other applications.[14] The primary raw material used in producing cellulose

[a] *Department of Chemical Engineering, Khalifa University of Science and Technology, P.O. Box 127788, Abu Dhabi, United Arab Emirates. E-mail: chandraverma.rs.apc@itbhu.ac.in, akram.alfantazi@ku.ac.ae*
[b] *Department of Chemistry, Udai Pratap (U.P.) Autonomous College, Varanasi 221002, India*

derivatives is wood cellulose, produced in millions of tons annually. Among the various cellulose derivatives, alkoxy celluloses have been most widely investigated and reported.[15] The word ''nanocellulose'' describes cellulose with a nanostructure. This could be microbial nanocellulose, which is a term for nano-structured cellulose made by bacteria, cellulose nanofibers (CNFs), also known as nanofibrillated cellulose (NFC), or cellulose nanocrystals (CNCs).[16] Nanosized cellulose fibrils with a high aspect ratio, *i.e.* length-to-width ratio, make CNF. Fibril lengths range widely, usually several micrometers, and their typical widths range from 5 to 20 nanometers. In addition, cellulose nanofibrils (CNFs) produced through homogenization, microfluidization, or crushing processes can be converted into highly crystalline, rigid nanoparticles, or nanocellulose, from native fibers by an acid hydrolysis process. These nanoparticles are shorter (100–1000 nanometers).[17] The substance that is produced is called cellulose nanocrystals (CNCs).

There are many uses for nanocellulose, from toys for kids to cleaning up oil spills.[18] The pharmaceutical, nourishment, and healthcare industries can all benefit from nanocellulose.[19] This new material is likely less expensive than most other high-performance nanoscale materials, and it can also replace some products based on petrochemicals.[20] Though one of the most rapidly expanding subfields in technological polymers is self-reinforced polymer composites, most of the materials used to develop these materials up to this point have been moderately effective thermoplastic fibers. Because of its high tensile strength and elastic modulus, natural cellulose may eventually replace glass fibers in specific applications. Compared to conventional fiber-reinforced plastics, cellulose composites create composites with greater fiber contents.[21] Furthermore, cellulose composites enable effective stress transfer and adhesion at their interface because these biocomposites' matrix and reinforcement phases are fully compatible. These cellulose composites can maintain the mechanical and thermal characteristics of the cellulose fibers under ideal processing conditions, and their superior interface can contribute to their optical transparency.[22,23] Various applications of cellulose and its organic and inorganic composites are illustrated in Fig. 3.

Chandrabhan Verma

Chandrabhan Verma works at the Department of Chemical Engineering, Khalifa University of Science and Technology, Abu Dhabi, United Arab Emirates. Dr. Verma obtained B.Sc. and M.Sc. degrees from Udai Pratap Autonomous College, Varanasi (UP), India. He received his PhD from the Department of Chemistry, Indian Institute of Technology (Banaras Hindu University) Varanasi, under the supervision of Prof. Mumtaz A. Quraishi in Corrosion Science and Engineering. Dr. Verma has three years of postdoctoral fellow (PDF) experience in the Department of Chemistry at North-West University, South Africa. He also has more than one year of postdoctoral fellow (PDF) experience in the Department of Advanced Materials, King Fahd University of Petroleum and Minerals (KFUPM). He is a reviewer and editorial board member of various internationally recognized ACS, RSC, Elsevier, Wiley and Springer platforms. Dr. Verma published numerous research and review articles in different areas of science and engineering at ACS, Elsevier, RSC, Wiley and Springer, etc. He has a total citation of more than 12200 with an H-index of 61 and an i-10 index of 157. His current research focuses on designing and developing industrially applicable corrosion inhibitors. Dr. Verma has edited/authored over 40 books for the ACS, Elsevier, RSC, Springer and Wiley. Dr. Verma received several awards for his academic achievements, including a Gold medal in M. Sc. (Organic Chemistry; 2010) and Best Publication awards from the Global Alumni Association of IIT-BHU (Second Prize 2013).

Vidusha Singh

Vidusha Singh is an assistant professor at the Department of Chemistry, Udai Pratap College, Varanasi, India. She is a research fellow at Udai Pratap College, Varanasi, India. She is pursuing her research in collaboration with the Institute of Sciences, Banaras Hindu University, Varanasi, India and Govt. V.Y.T. Post Graduate Autonomous College (govt. arts and science college) Chattisgarh, India. She has been teaching postgraduate and undergraduate classes in Chemistry for the last four years. Her research work is focused on material science and water purification.

1.2. Corrosion and corrosion control: a brief account on the contribution of carbohydrate polymers

Carbohydrate polymers are extended chains of monosaccharides connected by glycosidic bonds. Most living things serve as a significant food source and energy source. The type of monosaccharides determines whether they are homopolysaccharides or heteropolysaccharides. Linear polysaccharides are chains of monosaccharides; they can also be branched, referred to as a branched polysaccharide. They allow organisms to store energy. The molecules are hydrophobic because of their numerous hydrogen bonds, which prevent water from penetrating them.[25] They permit modifications to the concentration gradient, which affects how well the cells absorb water and nutrients. Glycolipids and glycoproteins are created when many polysaccharides form covalent bonds with lipids and proteins. The purpose of these glycolipids and glycoproteins is to transmit signals or messages both inside and between cells. Polysaccharide cellulose, which makes up the cell wall of plants, supports the cell wall. Chitin is essential for supporting the extracellular matrix surrounding cells in fungi and insects.[26] Carbohydrate polymers have potential applications in different fields, especially food applications.[27] Chemical functionalization can suitably tailor their properties, such as hydrophilicity, hydrophobicity, and applications (Fig. 4).[28] The hydrophilicity/hydrophobicity is an essential aspect of corrosion inhibitors as too high and too low hydrophilicity/hydrophobicity adversely affect the inhibition potential.

Akram AlFantazi

Akram AlFantazi is a Professor at the Department of Chemical and Petroleum Engineering and Theme Lead (Materials and Chemistry) at the Emirati Nuclear Technology Center (ENTC) at Khalifa University. He was a professor in the Materials Engineering Department and Founding Co-Director of the Pipeline Integrity Institute (PII) at the University of British Columbia (UBC), Vancouver, Canada. He also served as the Associate Dean of Research and Graduate Studies. Dr. Alfantazi has more than 350 publications, including 250 refereed journal publications. He has also co-edited several books. He has served as a consultant to various companies in the chemical, metallurgical, and petroleum industries. He is a Fellow of the Canadian Institute of Mining, Metallurgy and Petroleum, NACE International, and the Engineering Institute of Canada. He has received several awards for his work, including the Professional Engineers and Geoscientists of BC Teaching Award of Excellence, the Materials Society's Materials Scientists Distinguished Award and the Canadian Materials Chemistry Award. He was appointed a Chang Jiang Scholar at the China University of Mining and Technology.

Carbohydrate polymers have been widely used for their many benefits in developing green corrosion inhibitors, which can replace toxic chromates, nitrates, molybdates, tungstate, *etc*.based alternatives.[29–33] Over the past ten years, there has been a significant increase in enthusiasm for this class of compounds due to their biologically generated properties and the ability of some synthetic biopolymers, along with their products, to comply with environmental standards for safe product use, good corrosion inhibition potential, and negligibly small, reduced, or zero pollution risk.[29–33] They are a group of environmentally friendly, biodegradable, and chemically stable macromolecules with distinct inhibitory strength and mechanistic approaches to bulk and metal surface protection in corrosion inhibition.[29–33] Carbohydrate polymers isolated from natural sources (flowers, for example) can be upgraded to less expensive, renewable, and easily accessible substitutes that contain vital components that inhibit corrosion.[29–33] A variety of carbohydrate polymer series, comprising both homo- and heteropolysaccharides like chitosan, starch, cellulose, chitin, gum Arabic, and others, are extensively employed in long-term corrosion prevention.[29–34] Carbohydrate polymers are highly soluble in aqueous electrolytes, unlike conventional polymers. Nevertheless, issues with their solubility, stability, and additional refinement of their inhibitive qualities may still need to be improved using carbohydrate polymers as corrosion inhibitors.[35] More investigation and advancement are required to enhance the efficacy and suitability of carbohydrate polymers as corrosion inhibitors in various industrial settings.

Certain carbohydrate biopolymers typically possess distinct colloidal properties and a relatively high molecular mass.[25] The nature (structural and chemical properties) of the adsorption layers formed by certain carbohydrate biopolymers can play a significant role in determining their ability to inhibit associated cathodic reactions by blocking their active sites or limiting the rate of anodic dissolution by providing layers on the metal surface. In their interactions with metallic surfaces, the majority of carbohydrates can act as adsorption centers due to the presence of polar functional groups such as $-NH_2$, –OH, $-CH_2OH$, $-SO_3H$, $-COO^-$, $-NHCHCH_3$, –O– and $-COCH_3$.[29–34] Owing to their polymeric nature and abundance of adsorption sites, carbohydrate polymers should bind to the metallic surface to form a highly potent, chelating and persistent complex.[29–34] Furthermore, the polar functional groups of electrolytes may undergo deprotonation or protonation based on their specific type. Consequently, chemisorption and physisorption of carbohydrate polymers are possible on the surface of metals, with the physiochemisorption mechanism being the primary attachment mechanism.[29–34] The general requirements of a compound to be used as a corrosion inhibitor are schematically presented in Fig. 5. Carbohydrate polymer derivatization increases the number of adsorption centers and solubility of the polymers, increasing their inhibition potential. The polar functional groups, such as $-NH_2$, $-CH_2OH$, –OH, $-NHCOCH_3$, *etc.*, can serve as centers for derivatization. These functional groups aid in the distribution of active gradients in the polymer matrixes of composite coatings. Polar substituents

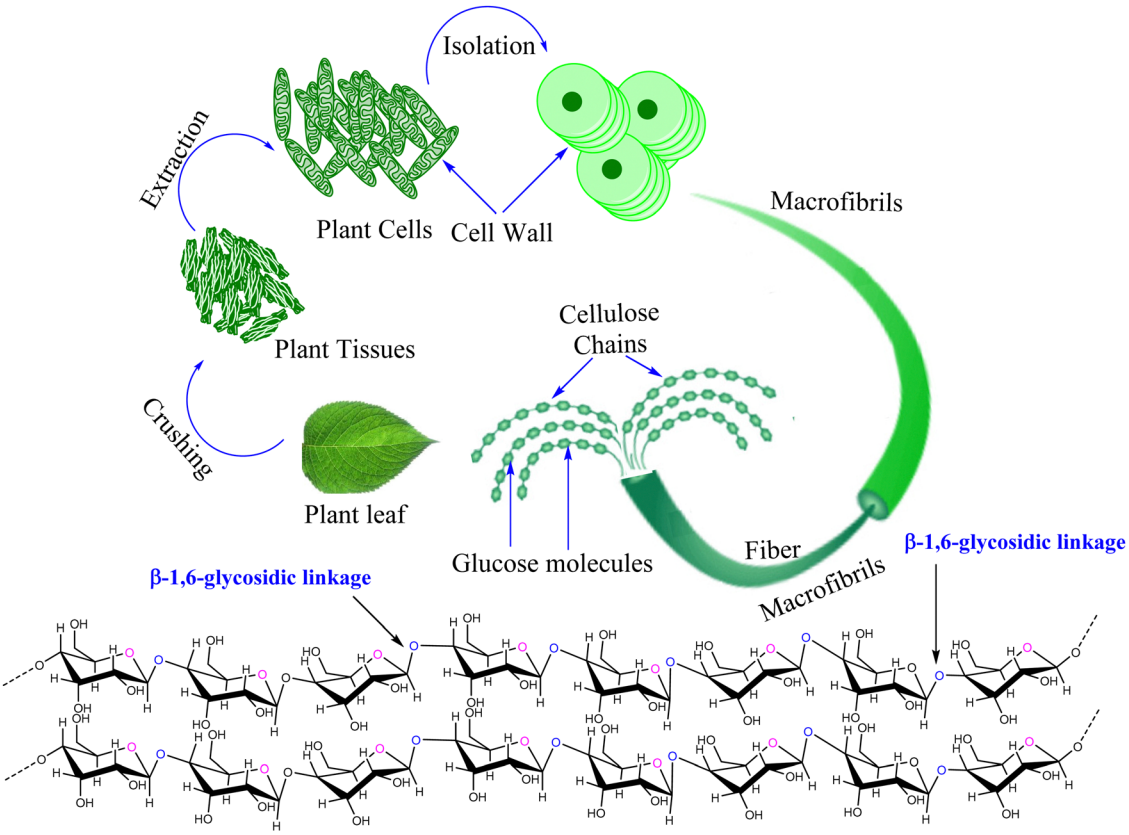

Fig. 1 Schematic illustration of the distribution of cellulose in plant tissue. (Self-illustration, Copyright permission is not required).

found in carbohydrate polymers and their derivatives can operate as adsorption sites when they come into contact with or connect with metal surfaces. These substituents further improve their solubility in the polar aqueous electrolytes.

1.3. What makes cellulose and its derivatives effective corrosion inhibitors?

Several benefits that improve the performance of cellulose and its suitability in a range of commercial and scientific uses come from functionalization, which is the process of adding functional groups to cellulose's chemical structure.[36] Regarding anticorrosive applications, cellulose composites and surface-functionalized materials are widely used. Functionalized cellulose is created by adding particular functional groups, such as –OH, $–NH_2$, –OR, *etc.*, to the cellulose backbone to change its chemical structure.[37] The distinct structural and chemical characteristics of cellulose make it a notably better inhibitor than other polysaccharides. The cellulose structure is inflexible and highly crystalline, consisting of linear chains of glucose molecules connected by β-1,4-glycosidic linkages. The corrosive and aggressive electrolyte species are unable to permeate and reach the metal surface due to the wide connection. This robust molecular arrangement creates a physical barrier to prevent enzymes and other molecules from accessing the cellulose substrate. Furthermore, the β-linkages in cellulose withstand hydrolysis better than the α-linkages in many other polysaccharides.[38] Because of its structural resilience, cellulose is less likely to be broken down by electrolytes and other corrosive species, making it a potent inhibitor of various corrosive environments. Cellulose and its derivatives exhibit remarkable inhibition potential due to its polymeric nature and multiple adsorption centers. The inhibition potential of functionalized cellulose is enhanced by the numerous beneficial aspects that come with chemical functionalization. The relative number of adsorption or coordination sites may rise in the presence of additional polar functional groups. The inhibition efficiency is increased due to the enhanced adsorption, which forms a more robust and protective layer for corrosive elements. Although cellulose itself can form chelating complexes, newly added functional groups can further improve the chelating capability of cellulose derivatives.[39,40] Because of their chelating qualities, certain functional groups, such as –OH, $–NH_2$, and –OR, can combine with metal ions to form complexes that prevent them from interacting with the metal surface.

Several isotherm models can be used to explain the nature and adsorption behavior of cellulose and its derivatives on metallic surfaces.[41,42] The adsorption isotherm study is essential to studying corrosion inhibition because it offers vital information on the interaction between corrosion inhibitors and metal surfaces.[43,44] A corrosion inhibitor's concentration and adsorption onto the metal surface are examined in

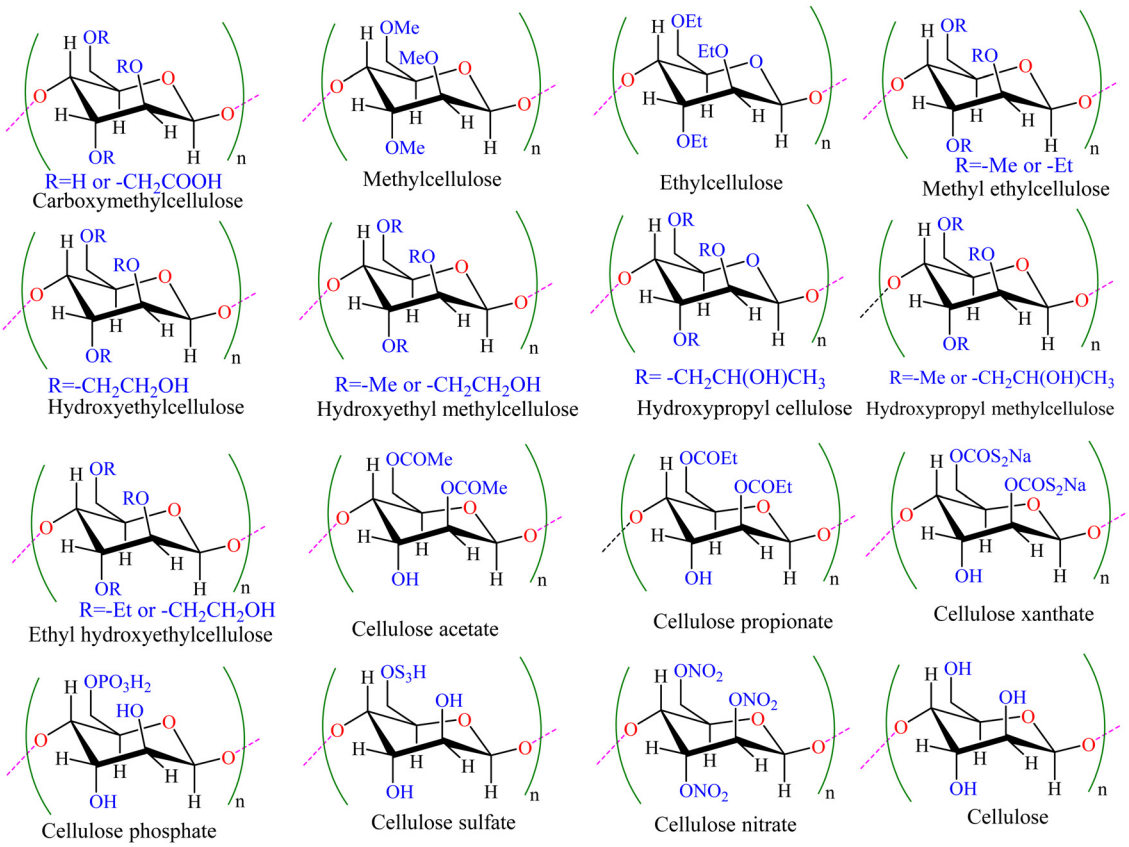

Fig. 2 Various derivatives of cellulose. (Self-illustration, Copyright permission is not required).

adsorption isotherm investigations, a subset of corrosion inhibition research. Finding significant variables like adsorption capacity, surface coverage, and the kind of adsorption model used is made possible by thoroughly understanding the adsorption isotherm.[43,44] These isotherm analyses offer vital new information about the effectiveness and mechanism of corrosion inhibition. The adsorption isotherm provides insight into the nature of the inhibitor-metal interaction by identifying the kind of adsorption, whether it adheres to the Freundlich, Langmuir, or other models.[45,46] To reflect the development of a protective layer on the metal surface, the Langmuir isotherm, for example, assumes monolayer adsorption with a defined capacity.[45,46] The Langmuir isotherm is one of the most studied and recorded isotherm models in adsorption. This model is useful in understanding the adsorption of a solution onto a surface since it has a finite number of identical, non-interacting adsorption sites. The Langmuir isotherm presumes monolayer adsorption, as there is only a chance that one layer of adsorbate molecules will form on the surface.[41,42] The maximal adsorption capacity and affinity of the adsorbent–adsorbate system, among other crucial parameters, can be ascertained using the Langmuir isotherm to comprehend the behavior of adsorption processes. Despite its widespread use, the Langmuir isotherm may not always accurately reflect the adsorption process; in these situations, alternative isotherm models, such as the Freundlich or BET models, may be more suitable.[47,48] The actual adsorption behavior may also differ from the assumptions made by the Langmuir model.

In addition, the extra functional groups in modified cellulose can be specially designed to give cellulose particular qualities like increased solubility, film-forming capability, and interaction with other additives.[49] Functionalized cellulose can adhere to metal surfaces more effectively and offer durable corrosion protection because of these specific properties. Cellulose has an extended chain of glucose units with many polar hydroxyl (–OH) functional groups. Under the influence of additives (synergists and antagonists) and electrolytes, these functional groups are readily subjected to physiochemical changes. Synergists and antagonists can be more noticeable in cellulose and its derivatives than in conventional corrosion inhibitors due to their comparatively higher number of functional groups.[29] Their biocompatibility, non-accumulative nature, biodegradability, and sustainability further contribute to the growing interest in cellulose and its derivatives for corrosion protection.[50] Cellulose also makes a significant contribution to anticorrosive coatings. Cellulose has been extensively used as a polymer matrix in such coatings, whereas cellulose nanocrystals (CNCs) and nanofibers (CNFs) are used as coating-reinforced materials.

The properties of cellulose, such as film-forming, adhesion, high mechanical strength, and high susceptibility to functionalization and chemical modification, have drawn interest in it

Fig. 3 Schematic illustration of the applications of (a) pristine nanocellulose[24] [Reproduced from ref. 24 with permission; Copyright@Wiley; 2023], (b) nanocellulose-based organic polymer composites[20] [Reproduced from ref. 20 with permission; Copyright@ACS; 2018] and (c) nanocellulose-based inorganic polymer composites[20] [Reproduced from ref. 20 with permission; Copyright@ACS; 2018].

as a possible polymer matrix for anticorrosive coatings.[51,52] The type of cellulose used, the composition of the coating, and the particular environmental conditions to which the coatings are exposed are some factors that affect cellulose's corrosion protection performance. Further developments in cellulose-based anticorrosive coatings are anticipated as this field's research and development continue, which could result in wider industrial adoption of these coatings across various industries. Reinforced anticorrosive coatings based on cellulose have several benefits over conventional coatings, making them a viable option for preventing corrosion in multiple sectors.[53] Improved mechanical strength, compatibility, adhesion and adsorption, tailored properties, lightweight and versatile nature, and eco-friendliness are undoubtedly linked to the addition of CNCs and CNFs.

Despite coming from natural resources and having valuable uses in various industries, including food, textiles, and pharmaceuticals, cellulose can be hazardous to human health and the environment.[11] The chemical procedures used to change cellulose frequently involve using solvents and chemicals that could be hazardous to the environment and human health.[54–56] If improperly handled, producing byproducts while synthesizing cellulose derivatives might contribute to environmental pollution. To tackle these issues, efforts are being made to create more environmentally friendly and sustainable synthesis techniques, implement green chemistry concepts, and investigate substitute sources of cellulose.[54–56] One of the most critical aspects of adequately developing these materials is balancing the functional advantages of cellulose derivatives and the requirement to reduce their potential toxicity.[57,58] Furthermore, the potential toxicity of some extraction techniques may come to light during the crucial phase of isolating cellulose from plant components to produce cellulose derivatives.[59,60] In conventional procedures, non-cellulosic components are broken down, and pure cellulose is extracted using strong chemicals such as acids and alkalis.[61,62] If not handled appropriately,

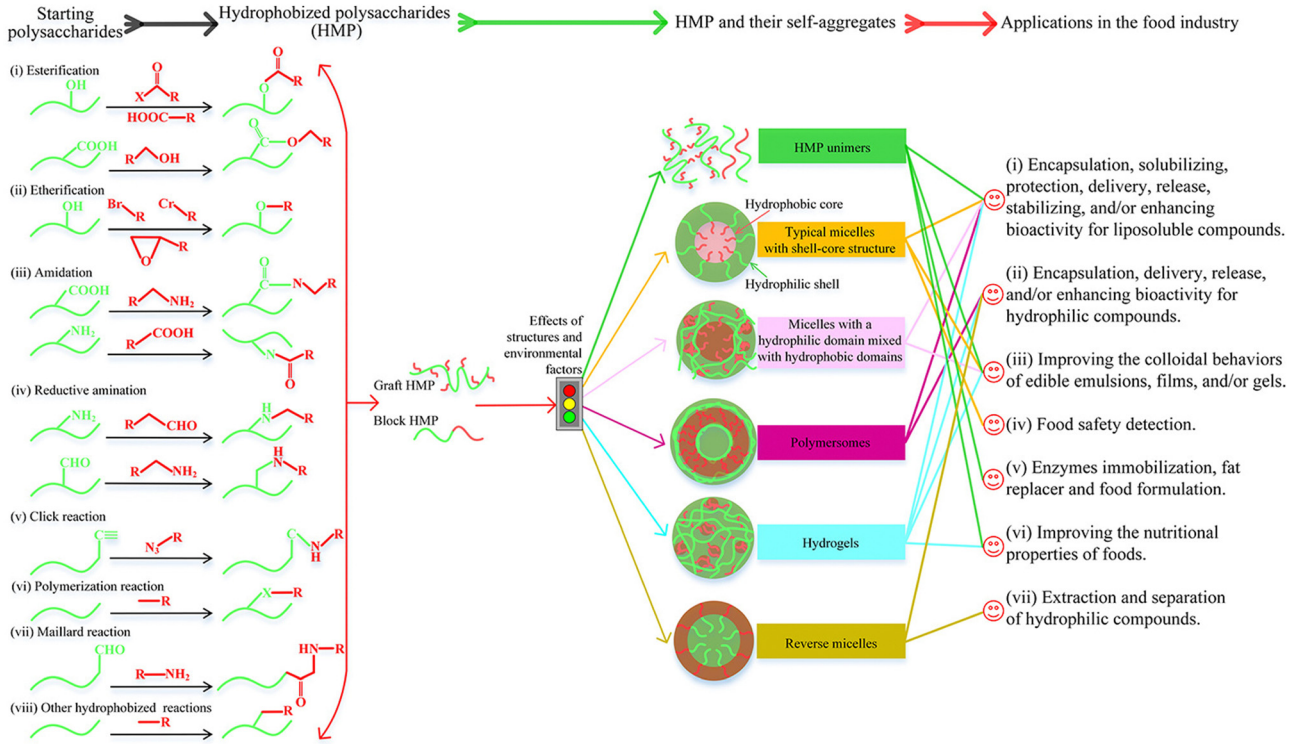

Fig. 4 Schematic illustration of the effect of hydrophobic modification on the properties and applications of carbohydrate polymers.[28] [Reproduced from ref. 28 with permission; Copyright@Elsevier; 2022].

these compounds can contribute to environmental pollution and endanger the health of those employed in the extraction process. Investigating new environmentally safe and sustainable isolation techniques, including enzymatic treatments and eco-friendly solvents, which try to reduce the usage of dangerous compounds, is one way to address these toxicity concerns.[61,62] Mitigating the possible negative impacts of generating cellulose-based materials on human health and the environment requires developing and implementing greener procedures in cellulose isolation.[63,64]

Chemically functionalized cellulose derivatives also manifest better anticorrosive activity in the coating phase.[65] Cellulose can be altered chemically to include functional groups that improve the polymer's compatibility with corrosion inhibitors.[66,67] Enhancing the adherence of corrosion inhibitors to the substrate surface by incorporating particular functional moieties on the cellulose backbone can result in higher inhibition efficiency. Furthermore, functionalized cellulose can offer greater film-forming and barrier qualities during the coating process, creating a more effective corrosion-protective film.[68,69] Optimizing the corrosion prevention effectiveness of coatings largely depends on the specific chemical alterations of cellulose, which also help make the coatings more durable and resilient in harsh environments. During the coating process, cellulose's chemical functionalization can improve the filler distribution's homogeneity. The naturally occurring polymer cellulose has hydroxyl groups on its surface that can be chemically altered to add particular functional groups.[70,71] The cellulose affinity for different coating materials and fillers can be enhanced by functionalizing the material's surface. Better cellulose-coating component adherence is facilitated by this change, which results in a more even dispersion of fillers throughout the coating matrix.[72,73] Functionalized cellulose can also be a compatibilizing agent, improving the interaction and dispersion of coating materials and fillers. The performance and characteristics of the coated material are ultimately enhanced by the chemical functionalization of cellulose, which also helps to increase homogeneity in filler distribution.[72,73] Cellulose derivatives such as methylcellulose and cellulose acetate are commonly utilized as film-forming agents during the coating phase due to their greater adherence and durability. These substances provide a stable, long-lasting coating immune to moisture and temperature fluctuations. The stability of cellulose and its derivatives in solution is influenced by solvent compatibility and molecular weight. Using the proper solvents and processing conditions is essential to maintaining the stability of cellulose derivatives in solution and preventing undesirable reactions or degradation. In general, an understanding of and emphasis on the stability of cellulose and its derivatives considerably enhances the efficacy and longevity of coatings in several applications, such as medications, food packaging, and cosmetics.

1.4. Effect of functionalization of cellulose and its derivatives: change in physiochemical properties and aqueous phase application

Functionalization of cellulose refers to introducing various functional groups or chemical moieties onto the cellulose

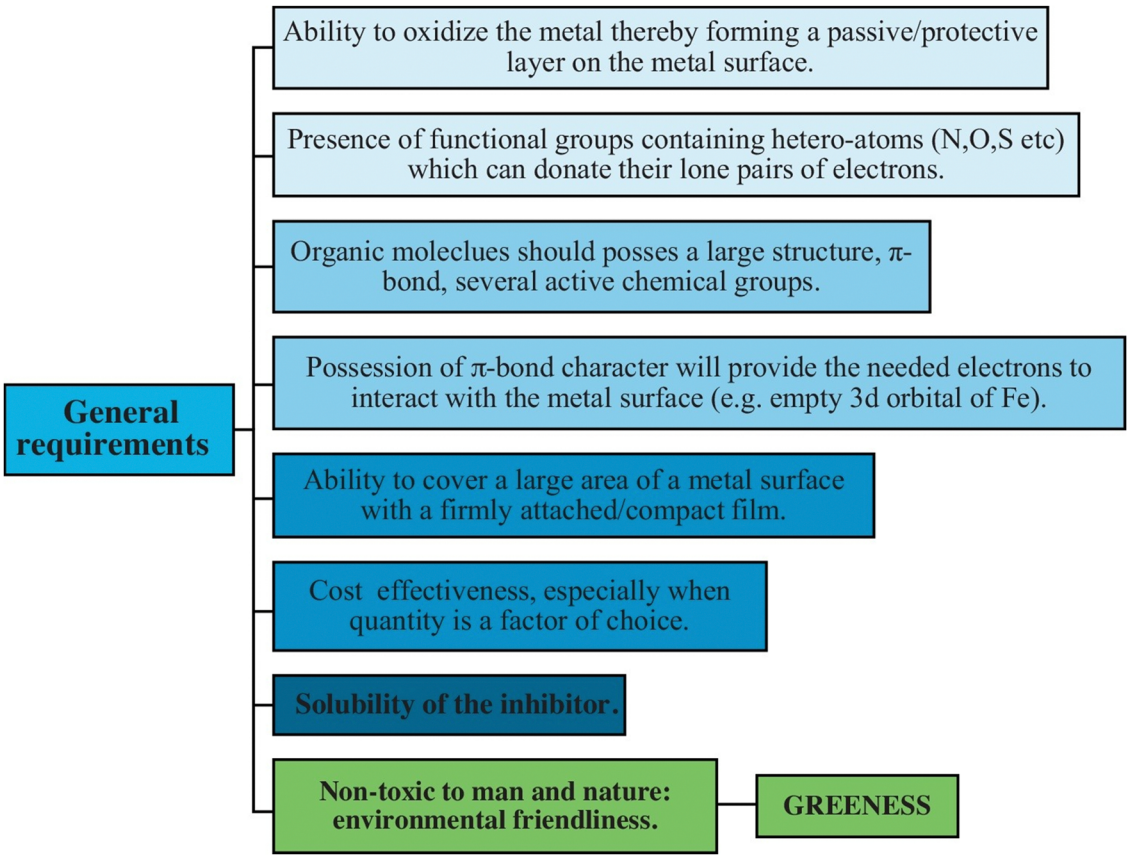

Fig. 5 Schematic presentation of the general requirements of a compound to be used as a corrosion inhibitor (left side)[29] [Reproduced from ref. 29 with permission; Copyright@Elsevier; 2016].

structure. This modification of cellulose can significantly alter its physiochemical properties, leading to enhanced or entirely new characteristics that can expand its potential applications, including corrosion protection.[74,75] One of the significant influences of chemical functionalization is enhanced solubility in polar electrolytes. Solubility is the most crucial requirement for aqueous phase application. The –OH at the C-3 position should be partially replaced to break the strong inter- and intramolecular hydrogen interactions and make the cellulose soluble in water or aqueous solutions.[76,77] This type of chemical modification alters the hydrophilic or hydrophobic derivatized cellulose. It is important to mention that a suitable combination of hydrophilicity and hydrophobicity is essential for a compound to be used as a corrosion inhibitor.[78,79] Being a biological macromolecule, cellulose is a temperature-sensitive polymer and undergoes degradation at high temperatures, limiting its industrial application.[80] Where corrosion is a significant challenge, most industries utilize highly aggressive electrolytes at high temperatures. Literature studies show that chemically modified cellulose manifests better (than pristine cellulose) thermal stability and could be used as a high-temperature corrosion inhibitor.[65,81] Furthermore, this chemical modification improves cellulose's mechanical strength, which is essential for practical anticorrosive coating applications.

Many computational studies, including DFT (density functional theory), MDS (molecular dynamics simulations), MCS (Monte Carlo simulations) and QSAR (quantitative structure–activity relationship), are widely used in describing the relative inhibition potential of different organic compounds, including polymers.[82,83] The criteria behind the computational studies are based on their relative chemical reactivity, *i.e.*, a more reactive compound is generally a more effective corrosion inhibitor. In cellulose-based anticorrosive coatings, the chemically modified CNCs and CNFs manifest better dispersibility in polymer matrixes.[84] Functionalization also improves the eco-friendliness of modified cellulose by increasing its biodegradability and compatibility.[85] In anticorrosive coatings where cellulose is used as a polymer matrix, some specific functional groups control the release of active substances, making functionalized cellulose suitable for corrosion inhibition and other controlled release applications such as drug delivery.[86,87] Furthermore, chemically modified cellulose manifests changed electrical conductivity. Electrical conductivity is another crucial aspect of anticorrosive coatings[88] for corrosion inhibition. To sum up, chemical functionalization is essential for improving the adsorption behavior, expanding the number of adsorption sites, promoting solubility, and raising the material's inhibitory efficacy in corrosion prevention applications. Functional groups or modifiers are added to its surface to improve the

material's ability to attract and interact with corrosive species. This alteration results in a more thorough covering of the material surface by increasing the number of adsorption sites accessible to inhibitor molecules and improving their binding affinity. Furthermore, the inhibitor's solubility is frequently enhanced due to the changed surface chemistry, which aids in its dispersion and efficient interaction with the corrosive medium. Together, these advancements improve inhibition efficiency and provide superior corrosion protection in various industrial-based electrolytes.

2. Cellulose and its derivatives in sustainable corrosion control: a literature survey

2.1. Chemically modified cellulose in sustainable corrosion control

Since cellulose is not well soluble in most commercially available electrolytes, little information is known about its use in aqueous phase corrosion inhibition. However, much research has been done on chemically modified cellulose in the aqueous phase for sustainable corrosion protection, particularly hydroxyethyl cellulose (HEC), carboxymethyl cellulose (CMC), and their modified derivatives.[81,88–98] Arukalam conducted a groundbreaking study using the weight loss method to examine the inhibitory effect of HEC for mild steel in 1 M HCl and 1.5 HCl.[99] The author observed that the %IE of HEC for MS corrosion increases with increasing concentration. HEC exhibits 69.61% and 58.14% efficiencies (at 2.5×10^{-3} M) in 1 M HCl and 58.14%, respectively. Mainly, HEC-based compounds act as mixed-type inhibitors, *i.e.* they possess compatibilities to retard both anodic and cathodic reactions.[100–102] They create a corrosion-inhibiting film by adsorbing using their e-rich sites. Although the Langmuir isotherm model was generally followed by their adsorption, some studies also reported the Frumkin isotherm.[100,101] Sangeetha *et al.* found that, as shown by scanning electron microscopy (SEM) and atomic force microscopy (AFM) analyses, aminated hydroxyethyl cellulose (AHEC) improves the surface morphology of corroded specimens through its adsorption (Fig. 6).[101] The aggressive attacks of corrosive ions and electrolytes severely corrode and damage the mild steel (MS) surface without AHEC.

A comparison of glucose, gellan gum, and hydroxypropyl cellulose in 1 M HCl to inhibit cast iron corrosion shows that modified cellulose is a more effective corrosion inhibitor than both substances.[102] Their %IE followed the sequence: C (89.6%) > B (80.9%) > A (69.5%). Furthermore, investigation and development show that the %IE of HEC depends upon the nature of the electrolyte and metal/alloys under investigation. Arukalam *et al.*[103] demonstrated that HEC manifests relatively more %IE (93.61%) at lower concentration (1500 ppm) for MS in 0.5 M H_2SO_4 than for Al. For Al, HEC shows 64.18% efficiency at concentrations as high as 2000 ppm. Another report indicates that HEC demonstrates 95% in 1 M HCl at 2000 ppm and 96% in 0.5 M H_2SO_4 at only 1000 ppm.[104] A similar observation was reported for mild steel corrosion in 1 M HCl and 0.5 M H_2SO_4.[105] Regarding the potential of cellulose

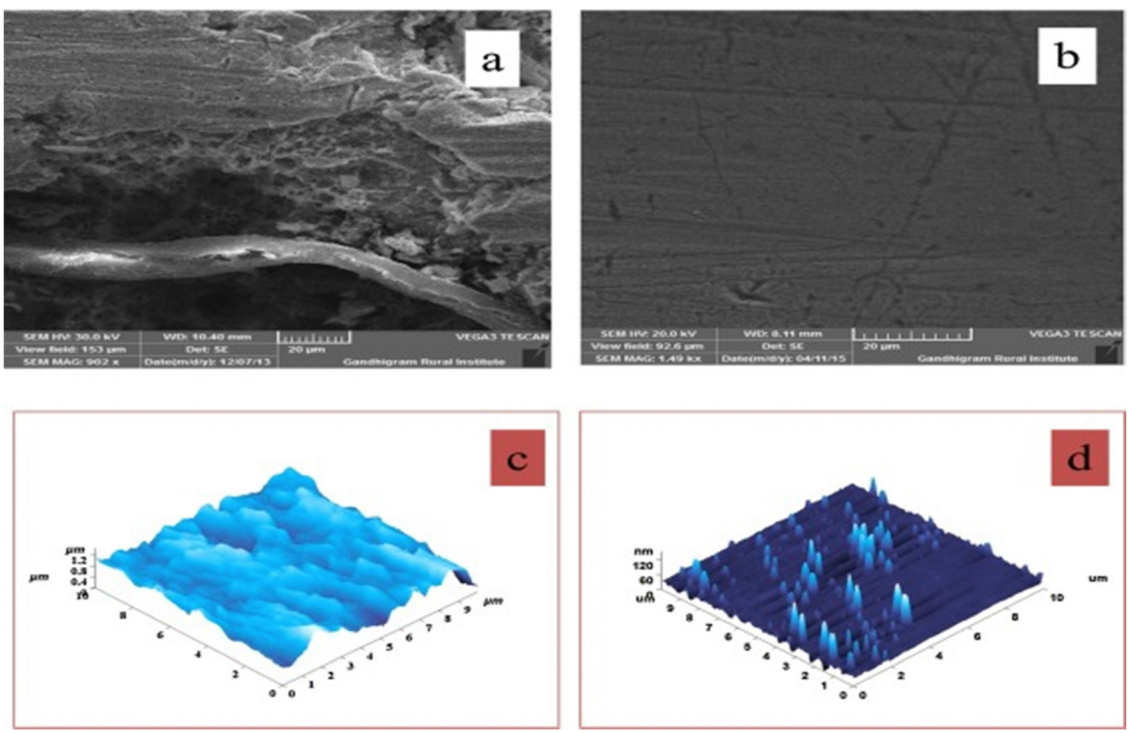

Fig. 6 (i) SEM and (ii) AFM pictures of mild steel specimens that are (a, c) uninhibited and (b, d) inhibited by AHEC[101] [Reproduced from ref. 101 with permission; Copyright@Elsevier; 2016].

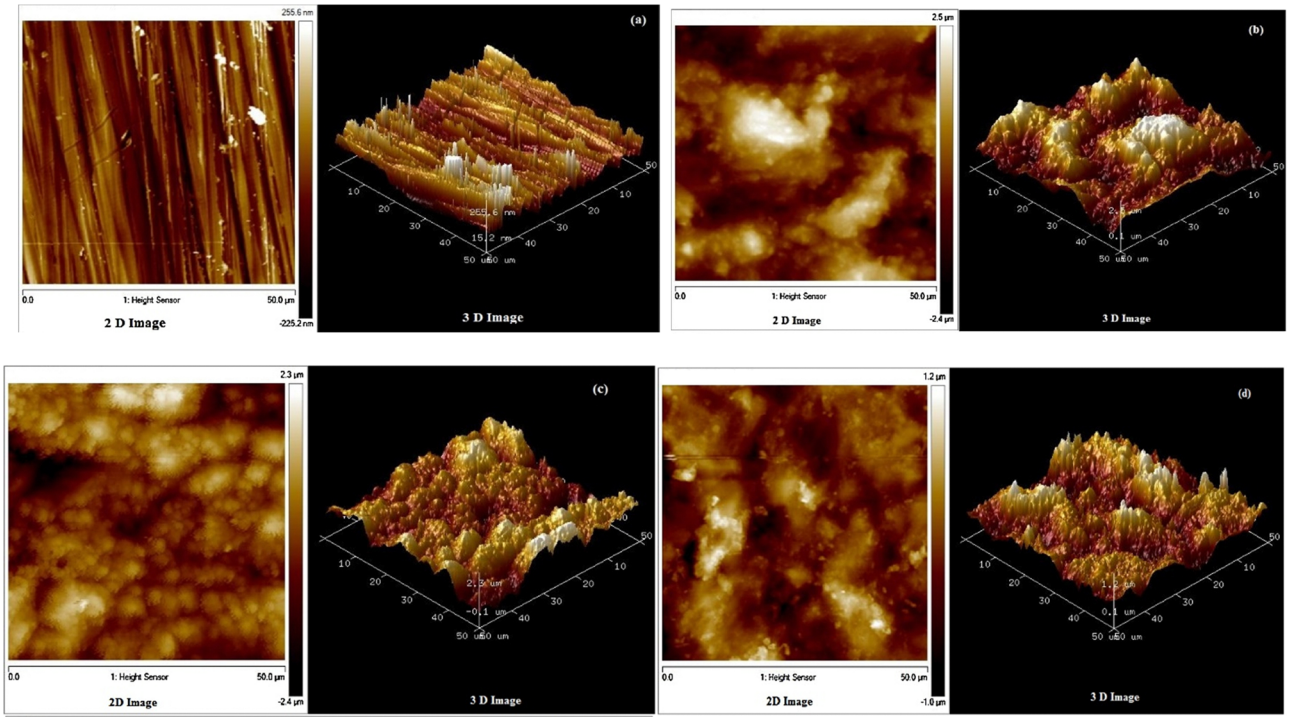

Fig. 7 2D and 3D AFM images of CS submerged in 1 M HCl for 6 hours at 30 °C with and without inhibitors. The specimens are presented as follows: (a) polished; (b) uninhibited in 1 M HCl; (c) inhibited in 1 M HCl with 500 ppm HEC. (d) The specimen was incubated in 1 M HCl containing 500 ppm HEC and 5 ppm TX[109] [Reproduced from ref. 109 with permission; Copyright@Elsevier; 2016].

derivatives to prevent corrosion, the phenomenon of synergism, or synergistic effect, has also been thoroughly investigated and documented.[106–110] The term ''synergistic effect of corrosion inhibitor'' describes combining two or more ingredients to produce an inhibitory effect on corrosion higher than the total components applied individually.[29] The outcomes of a study indicate that ethyl hydroxyethyl cellulose (EHEC) manifests only 55.64% efficiency for the MS/0.5 M H_2SO_4 system for two days of immersion time. However, potassium iodide (KI) improves the %IE up to 63.28%.[106] A similar observation was also derived for mild steel corrosion inhibition in 0.5 M H_2SO_4 using hydroxypropyl methylcellulose (HPMC) and KI.[107] For zinc–carbon electrodes in 26% NH_4Cl solution that is utilized in battery applications, HEC is also employed as a corrosion inhibitor.[108] At 300 ppm, it exhibits an efficiency of 92.07%. The polarization study suggests HEC's mixed-type behavior. The adsorption of HEC on the electrode in such electrolyte followed the Langmuir isotherm model. Mobin and Rizvi studied the inhibition effect of HEC with and without surfactants for A1020 CS corrosion in 1 M HCl using chemical, electrochemical, surface and computational techniques.[109] The comparative impact of three surfactants, sodium dodecyl sulfate (SDS), Triton X 100 (TX), and cetyl pyridinium chloride (CPC), was shown at various HEC concentrations. According to weight loss and electrochemical research results, the inhibitory performance of HEC is significantly enhanced by the presence of SDS, TX, and CPC. TX exhibits the greatest synergistic effect on HEC inhibition efficiency, followed by CPC and SDS, in that order. HEC inhibits corrosion by adsorbing at the surface of the metal as the surfaces become smoother in the presence of HEC, especially in the presence of TX, as seen by AFM images in Fig. 7. The average surface roughness (R_a) of polished, corroded, inhibited by 500 ppm HEC and inhibited by 500 ppm HEC + 5 ppm TX were 71.4, 627, 489 and 290 nm, respectively. Scanning electron microscope (SEM), energy dispersive X-ray (EDX), and UV-visible (UV-vis) spectroscopic measurements also support the adsorption mode of corrosion protection. Other studies also document the corrosion inhibition potential of cellulose derivatives.[111,112]

Farhadian *et al.* synthesized a polyurethane modified HEC (CHEC) to improve the %IE of HEC and studied its inhibition performance for MS in a pickling solution (15% HCl).[65] The CHEC was synthesized by the previously reported method as per Scheme 1. First, PEG 1500 (0.046 mol) was added to a 500 mL flask after being dissolved in 100 mL DMF. After being stirred for 30 minutes, the reaction temperature was increased to 60 °C. The polyurethane prepolymer was then prepared by adding 0.055 mol of methylene diphenyl diisocyanate (MDI) dissolved in DMF to the solution and stirring the mixture for three hours. Subsequently, 200 mL of DMF-dissolved HEC (7.5 g) was added to the mixture, and the reaction continued for 12 hours. The corrosion inhibition studies used the following techniques: weight loss (WL), open circuit potential (OCP), electrochemical impedance spectroscope (EIS), potentiodynamic polarization (PDP), scanning electron microscope (SEM), atomic force microscope (AFM), X-ray

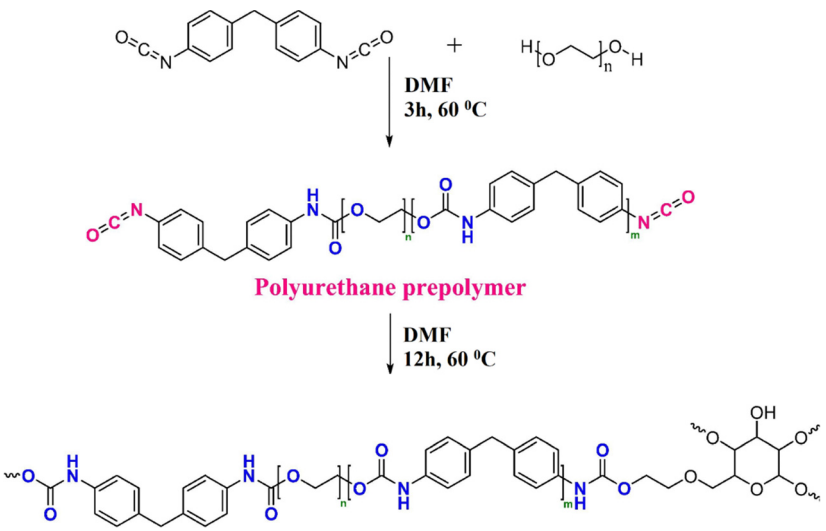

Scheme 1 Schematic illustration of the CHEC synthesis[65] [Reproduced from ref. 65 with permission; Copyright@Elsevier; 2021].

photoelectron spectroscopy (XPS), density functional theory (DFT), and molecular dynamics (MD) simulations. In line with WL studies, a rise in CHEC concentration increased the surface coverage and inhibition efficiency while decreasing the corrosion rate. The 50 and 6 mM concentrations produced the highest (94%) and lowest (82%) inhibition efficiencies of CHEC, respectively. In the system with 50 mM CHEC, the corrosion rate decreased from 128.5 mm year^{-1} in the blank solution to 7.9 mm year^{-1}.

Compared to the blank solution at 20–60 °C, including CHEC in the 15% HCl solution resulted in a possible shift toward more positive values. This suggests that CHEC improved the metal surface's luster by stabilizing the corrosion product at the interface. In contrast to an uninhibited solution, regardless of temperature, adding CHEC to the acid solution decreased the current densities of the polarization reactions. The metal dissolution and hydrogen evolution reaction rates appear to have been suppressed by CHEC. The Nyquist plots demonstrate depressed capacitive circular shapes with just one time constant, which suggests charge transfer influence on the corrosion process (Fig. 8). Furthermore, as the CHEC concentration rose, the Nyquist plots in the CHEC solution showed a larger diameter than the blank. This may be connected to CHEC's anticorrosion action, which strengthens the MS surface's resistance to corrosion. In the Bode phase angle diagrams, the single peaks are observed as a one-time constant for both the acid corrodent with and without CHEC. More significant and broader spikes in the presence of CHEC indicate a relaxation effect brought on by the MS surface's creation of a barrier layer. DFT and MDS-based computational studies provide good support for experimental studies.

Carboxymethyl cellulose (CMC) is one of the cellulose derivatives that contributes significantly to long-term, sustainable corrosion protection in the aqueous phase. Its high efficiency typically results from comparatively high concentrations or the presence of an appropriate synergist. Using weight loss and hydrogen evolution methods at different temperatures (30–60 °C), Umoren and colleagues examined the corrosion and corrosion inhibition effect of CMC for mild steel in a sulfuric acid medium (2 M H_2SO_4).[110] The %IE rises as the immersion time increases but falls as the temperature rises. Cl^- and I^- ions produce antagonistic and synergistic effects on the inhibition effect of CMC, respectively. The Langmuir adsorption isotherm model was discovered to describe the adsorption of CMC molecules onto the mild steel surface in both the presence and absence of halide ions. The WL and HE studies were used in another study to describe the %IE of CMC for mild steel in 2 M HCl solution.[113] The results of another survey of CMC's groundwater-based carbon steel corrosion inhibition effect show that the presence of Zn^{2+} cations enhances CMC's inhibition capacity.[114] The highest %IE of 48% is shown by CMC at 250 ppm concentration; however, at the same concentration, its %IE increases to 98% in the presence of 50 ppm of Zn^{2+} ions.

Umoren *et al.* found that CMC is a better corrosion inhibitor than chitosan (Ch), but less effective than commercial inhibitors when examining the inhibition effect of CMC for API 5L X60 pipeline steel corrosion in CO_2-saturated 3.5% NaCl.[115] The EIS research shows that once the amounts of all three inhibitors rise, so does the diameter of the Nyquist curves (Fig. 9). The three tested inhibitors' Nyquist plots have similar shapes, which suggests that their protective mechanism remained constant as the concentrations rose. In this study, greater concentrations of these inhibitors have wider Nyquist curve widths, indicating concentration dependence on the corrosion process. Larger diameters of the Nyquist semicircles are characteristics of higher corrosion resistance systems of inhibitors compared to the blank solution. In the presence and absence of the optimal (100 ppm) CMC, Ch, and commercial inhibitor's concentrations, these authors observed similar findings and trends of %IE when conducting corrosion tests at 25, 40, and 60 °C. The increase in the

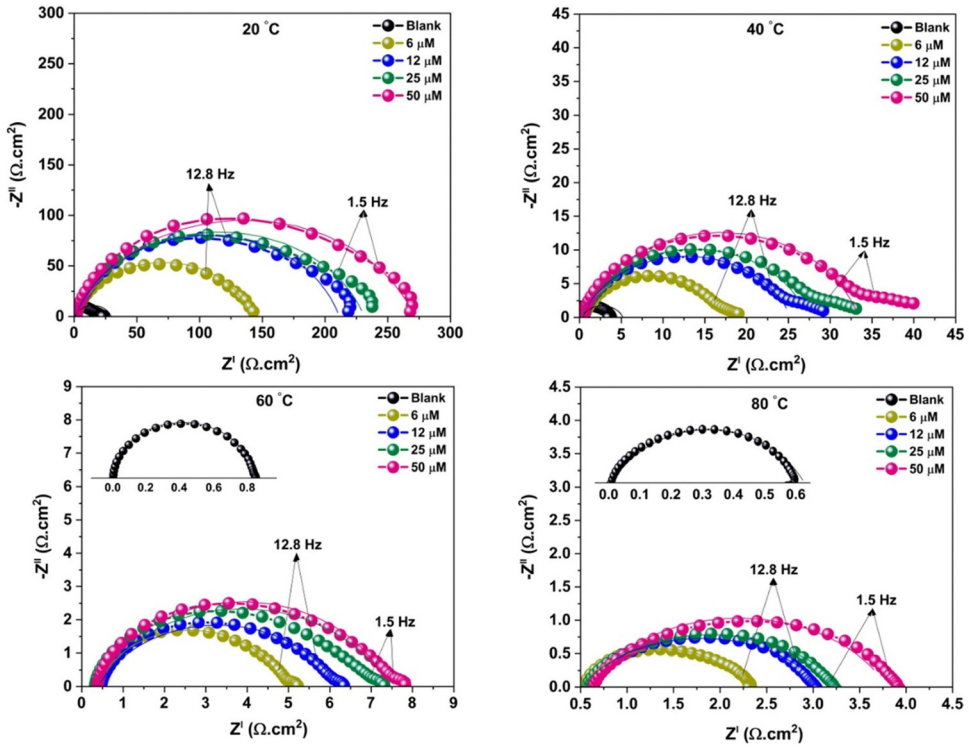

Fig. 8 Nyquist graphs for MS in the 15% HCl medium, with and without different CHEC concentrations at 20 °C, 40 °C, 60 °C, and 80 °C[65] [Reproduced from ref. 65 with permission; Copyright@Elsevier; 2021].

diameter of the Nyquist curves follows the same trend (Fig. 10). A different study shows that adding PVAc (polyvinyl acetate), PVP (polyvinylpyrrolidone), and PAA (polyacrylic acid) enhances CMC's ability to inhibit carbon steel corrosion at 1 M HCl and 1 M KOH.[116] In acidic solutions, CMC is also used to prevent the corrosion of copper, aluminum, and mild steel.[51,117–122] The CMC typically becomes effective by adhering to the metallic surface as described by the Langmuir isotherm model. CMC is a mixed-type corrosion inhibitor because its presence alters the anodic and cathodic Tafel curves. A summary of studies on the inhibition potential of HEC and CMC-based corrosion inhibitors is illustrated in Table 1.

2.2. Nanocellulose and cellulose composites in sustainable corrosion control

2.2.1. Nanocellulose and cellulose composites as corrosion inhibitors in the aqueous phase. There has been a notable surge in research interest regarding the synthesis, characterization and applications of cellulose composites (CCs).[123–126] Composites are made of a polymer matrix and are meant to be used as reinforcement. Because traditional fibers are becoming more affordable, there is a growing need for environmentally friendly materials. These kinds of composites are used with hindered natural fibers, which makes moisture absorption inherent. Recently, cellulose composites have been utilized to improve the assimilation of inorganic materials in various fields with multi-functional properties, such as fibers, aerogels, hydrogels and packaging.[127] Their biodegradable, renewable, non-corrosive, and high strength-to-weight ratio qualities also increase their applications in household, automotive, and aerospace products.[128,129] There is a paucity of research regarding their ability to prevent corrosion in the aqueous phase. A few studies demonstrate that, when applied in an aqueous phase, CCs effectively inhibit corrosion.

Solomon *et al.* synthesized CMC and silver nanoparticle-based composites (CMC/AgNPs) and used them as effective corrosion inhibitors for St37 steel in 15% H_2SO_4.[130] The synthesized CMC/AgNPs were characterized by transmission electron microscopy (TEM), SEM, EDX, Fourier transform infrared (FTIR) and UV-vis methods and their inhibition effect was measured by various techniques. A concentration of 1000 ppm of CMC/AgNPs provides an optimal inhibition efficiency of 93.94% at 25 °C. At 60 °C, a weight loss method has demonstrated an inhibition efficiency of 96.37%. The Langmuir adsorption isotherm explains the adsorption, and it is discovered that CMC/AgNPs slow down both the anodic and cathodic reactions. The surface of the St37 sample in the acid solution with the inhibitor is smoother than in the solution without the inhibiting agent, according to AFM and SEM graphics. The metal surface has adsorbed CMC/AgNPs molecules, according to FTIR and EDS data. Hasanin and Kiey developed a microcrystalline cellulose–niacin composite (NMCC) and carboxymethyl cellulose–niacin composite (NCMC) as aqueous phase corrosion inhibitors for copper in 3.5% NaCl.[131] With the aid of FTIR, thermogravimetric analysis (TGA), dynamic light scattering (DLS), SEM and EDX, NMCC and NCMC were described. At

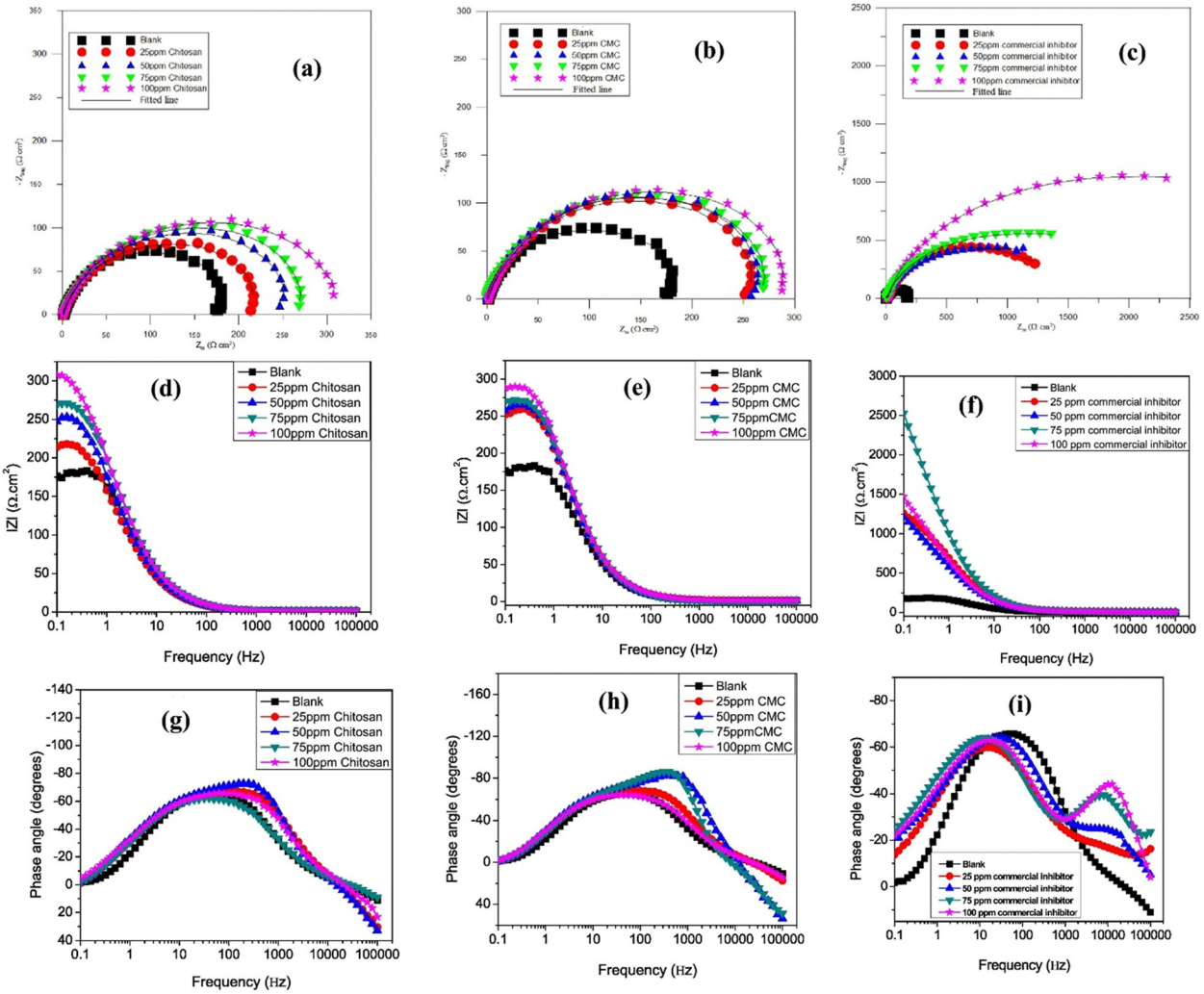

Fig. 9 API 5L X60 steel impedance plots in a CO_2-saturated 3.5% NaCl solution with and without different commercial inhibitors, chitosan, and CMC concentrations in (a–c) Nyquist, (d–f) Bode frequency, and (g–i) Bode phase angle representations at 25 °C[115] [Reproduced from ref. 115 with permission; Copyright@Elsevier; 2018].

100 ppm concentration, NMCC and NCMC exhibit the best %IEs of 33.2% and 83.4%, respectively.

Lateef *et al.* synthesized carboxymethyl cellulose/metal (Cu, Fe and Ni) composites, designated as CMC/Cu NP, CMC/Fe NP and CMC/Ni NP, and evaluated their %IE for carbon steel in 2 M HCl.[132] The best %IE of 98.4%, 96.2%, 94.9% and 76.6% was derived for CMC/Ni NP, CMC/Cu NP, CMC/Fe NP and CMC, respectively, at their optimum concentration (400 ppm). Surface analyses verified that the manufactured nanocomposites could effectively thwart a forceful attack. This group of authors also synthesized, characterized and evaluated the inhibition potential of CuO@MEL@CNCs (copper oxide/melamine/cellulose nanocrystals) and NiO@MEL@CNCs (nickel oxide/melamine/cellulose nanocrystals) for AISI360-steel corrosion in 1.0 M H_2SO_4.[133] The inhibition effect of CuO@MEL@CNCs and NiO@MEL@CNCs was compared with the efficiency of CNCs (cellulose nanocrystals). Electrochemical analyses suggest a significant improvement in the %IE of CNCs derived after the composite formation. OCP study indicates that CNCs, CuO@MEL@CNCs and NiO@MEL@CNCs successfully replaced the oxide layers from the surface and built a corrosion protective film.

PDP study was conducted in the absence and presence of 10, 40 and 75 ppm concentrations of CNCs, CuO@MEL@CNCs and NiO@MEL@CNCs. It was derived that the presence of the CNCs and their composites causes a significant change in the anodic and cathodic Tafel curves (Fig. 11). The presence of CNCs, CuO@MEL@CNCs, and NiO@MEL@CNCs significantly reduced the corrosion current density values, suggesting that they prevent aggressive electrolyte attacks and block corrosion-related active sites. The same concentrations of CNCs, CuO@MEL@CNCs, and NiO@MEL@CNCs were used in the EIS study to explore corrosion prevention's adsorption mode better. Fig. 12 shows the Nyquist plots for ISI360-steel corrosion in 1.0 M H_2SO_4 solution in the absence (blank) and presence of different concentrations of CNCs, CuO@MEL@CNCs, and

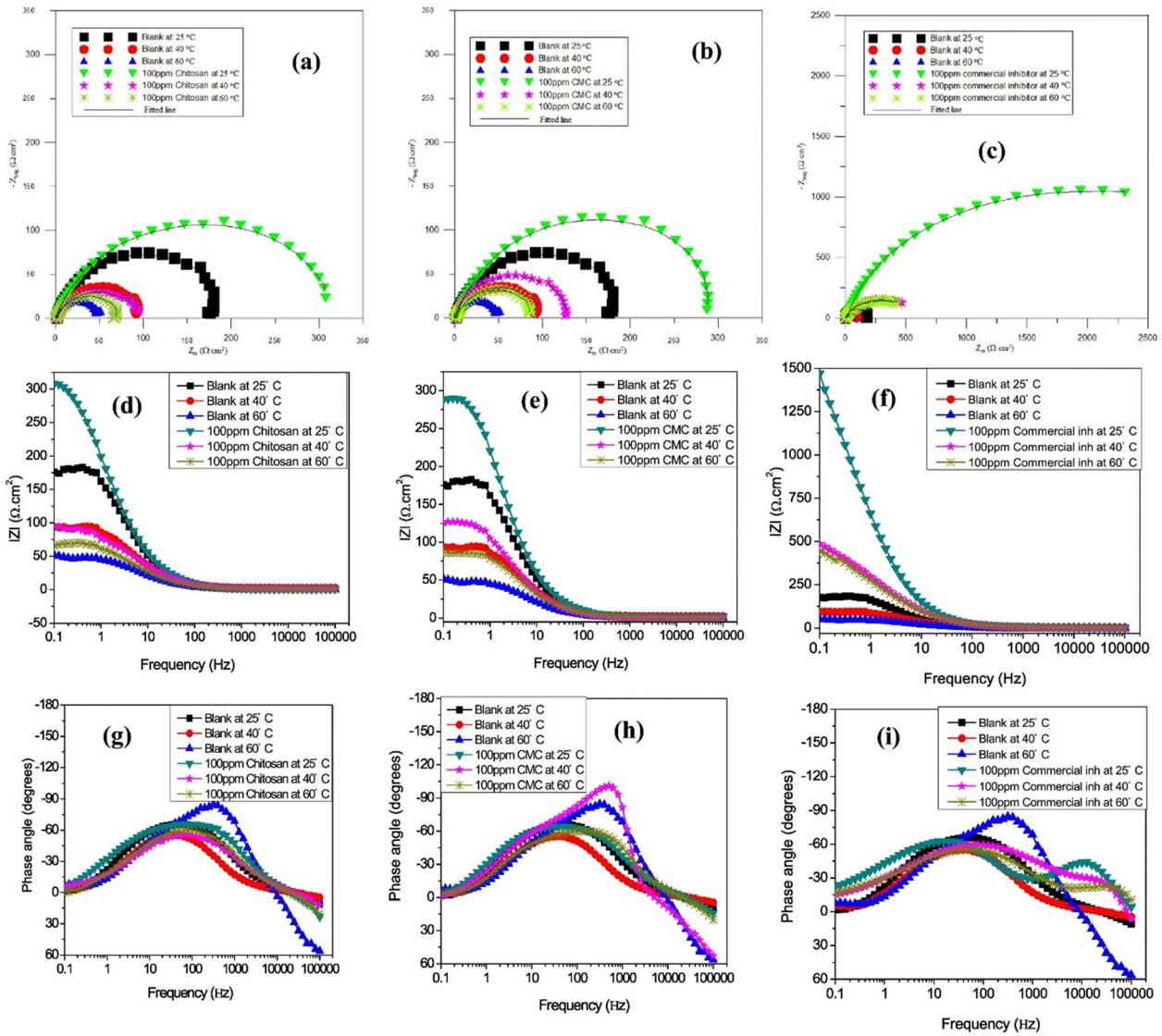

Fig. 10 API 5L X60 steel impedance plots in a CO_2-saturated 3.5% NaCl solution with and without 100 ppm of commercial inhibitor, chitosan, and CMC at different temperatures represented by (a–c) Nyquist, (d–f) Bode frequency, and (g–i) Bode phase angle representations[115] [Reproduced from ref. 115 with permission; Copyright@Elsevier; 2018].

NiO@MEL@CNCs. The Nyquist diagrams for the inhibitor-containing and blank systems revealed depressed semicircles, indicating a high degree of similarity in the AISI360-steel corrosion mechanism across all systems. The addition of inhibitors significantly increased the semicircle size and polarization resistance, according to a careful analysis of the Nyquist profiles. This indicated that the inhibitors adsorbed on the AISI360-steel surface, forming a protective film at the electrode/solution interface of the material.

These authors also described the relative performance of nanocrystalline cellulose (NCC) for SS316 Alloy corrosion inhibition in 2 M HCl, having developed NCC by acid hydrolyzing macrocrystalline cellulose (CEL).[134] The results obtained from the different empirical approaches were compared and showed that these polymers' protective effectiveness increased with an increase in concentration in the following order: CEL (93.1%) < NCC (96.3%). By impeding the active centers on the metal interface, the studied polymers exhibit mixed-corrosion features, and their adsorption follows the Langmuir isotherm model. The presence of inhibitors (CEL and NCC) decreases the corrosion current density in the Tafel curves and increases the diameter of the Nyquist curves and charge transfer resistance (Fig. 13). SEM surface morphological investigations supported the polymer binding on the metal substrate. The DFT parameters displayed the anti-corrosive properties of the CEL and NCC polymers, which were as anticipated. According to a Monte Carlo (MC) simulation study, the CEL and NCC polymers are firmly adsorbed on the surface of the SS316 alloy, creating a potent protective layer. Recently, Lu *et al.* studied the inhibition potential of carboxymethyl cellulose and polyaniline composites (PANI/CMC composites) for Q235 steel corrosion in 1 M HCl.[135] The findings demonstrate the good inhibitory features

Table 1 A summary of significant reports on hydroxyethyl cellulose (HEC) and carboxymethyl cellulose (CMC) based corrosion inhibitors in the aqueous phase

Nature of cellulose derivative	Nature of metal/electrolyte	Nature of inhibitor/ adsorption	Best %IE/optimum conc.	Techniques of study	Salient feature(s)	Ref.
Hydroxyethyl cellulose (HEC)	Mild steel/1 M and 1.5 M HCl	—	69.61% (1 M HCl) and 58.14% (1.5 M HCl)/2.5 × 10^{-3} M	WL.	With increased HEC concentration, θ and %IE rise. The rate at which corrosion occurs increases with HCl concentration.	99
Hydroxyethyl cellulose (HEC)	A1020 carbon steel/1 M HCl	Mixed-type/Frumkin isotherm	91.8%/900 ppm	WL, EIS, PDP, FTIR, XRD, SEM and AFM.	The WL demonstrated that as AHEC conc rose, so did %IE. FTIR and XRD studies validated the AHEC's adsorption.	100
Aminated hydroxyl ethyl cellulose (AHEC)	Mild steel/1 M HCl	Mixed-type/Frumkin isotherm	96.7%/0.5 mM	EIS, PDP, SEM, EDX and DFT.	Results showed that HEC conc. rose, and so did %IE. It becomes effective by developing the inhibitive film.	101
Hydroxypropyl cellulose (HPC)	Cast iron/1 M HCl	Mixed-type/Langmuir isotherm	89.6%/500 ppm	WL, EIS, PDP, FTIR, XRD and SEM.	The %IEs of glucose (A), gellan gum (B) and HPC (C) followed the order: C (89.6%) > B (80.9%) > A (69.5%).	102
Hydroxyethyl cellulose (HEC)	Mild steel & aluminium/0.5 M H_2SO_4	Mixed-type (MS) & cathodic-type (Al)/Langmuir isotherm	93.61% (MS)/1500 ppm & 64.18% (AL)/2000	WL, PDP, EIS, DFT and MDS.	As per the PDP study, HEC primarily inhibited the cathodic reaction of Al, but it is a mixed-type inhibitor for MS corrosion.	103
Hydroxyethyl cellulose (HEC)	Copper/1 M HCl and 0.5 M H_2SO_4	Exhibits passive behavior	95% (1 M HCl)/2000 ppm & 96% (0.5 M H_2SO_4)/1000 ppm	WL, EIS, PDP, DFT and MDS.	EIS studies show that HEC was adsorbed on the Cu surface but did not affect the corrosion mechanism. HEC adsorption was enhanced by adding KI, which did not affect the HEC inhibition mechanism.	104
Hydroxypropyl methylcellulose (HPMC)	Mild steel/1 M HCl and 0.5 M H_2SO_4	Mixed-type/Langmuir isotherm	90.92% (0.5 M H_2SO_4) and 90.48% (1 M HCl)/2000 ppm	WL, EIS, PDP, DFT and MDS.	EIS verifies that HPMC was adsorbed on the metal surface. HPMC was adsorbed on the mild steel surface *via* the hydroxypropoxy end of the molecule and the aromatic ring to form a protective layer.	105
Ethyl hydroxyethyl cellulose (EHEC)	Mild steel/0.5 M H_2SO_4	Cathodic-type/Langmuir isotherm	61.81%/2.5 g L^{-1} EHEC + 2.5 g L^{-1} KI	WL, EIS, PDP and DFT.	The protonated and neutral species create the surface chemisorbed film. EHEC and EHEC + KI demonstrated a cathodic effect. The structure of the molecules influences the efficiency of inhibition.	106
Hydroxypropyl methylcellulose (HPMC)	Mild steel/0.5 M H_2SO_4	Cathodic-type/Freundlich isotherm	94.02%/2000 mg L^{-1} HPMC + 500 mg L^{-1} KI (5 days)	WL, EIS, PDP and DFT.	The inhibitory effectiveness of HPMC was enhanced by KI working in concert. HPMC molecules corrode quickly on metal surfaces.	107
Hydroxyethyl cellulose (HEC)	Zinc–carbon battery/26% NH_4Cl	Mixed-type/Langmuir isotherm	92.07%/300 ppm	PDP, EIS, SEM and FTIR.	Due to adsorption, HEC provides protection. The adsorption mode followed physiochemisorption. Using SEM in conjunction with FTIR analysis, the adsorption layer is HEC.	108
Hydroxyethyl cellulose (HEC)	A1020 carbon steel/1 M HCl	Anodic-type/Langmuir isotherm	91.62%/500 ppm + 5 ppm TX.	WL, EIS, PDP, UV-vis, SEM, EDX, AFM and DFT.	The synergistic effect followed the order (500 ppm HEC): 5 ppm TX (91.62%) > 5 ppm CPC (91.07%) > 5 ppm SDS (90.77%).	109
Methyl hydroxyethyl cellulose (MHEC)	Copper/1 M HCl	Mixed-type/Langmuir isotherm	90.29%/4 g L^{-1}	WL, PDP and SEM.	The inhibition action results from the MHEC adsorption on the Cu surface, which blocks the transfer of mass and charge and protects the copper surface from harmful ions.	111
Hydroxyethyl cellulose (HEC)	Stainless steel AISI 304 welded pipe/3.5% NaCl and turbulent flow.	—	65.95%/600 ppm	EIS, PDP and SEM.	The rate of corrosion rises as the turbulent flow does. With a scanning electron microscope, pitting corrosion on the welding pipe's heat-affected zone can be seen.	112
Modified hydroxyethyl cellulose (CHEC)	Mild steel/15% HCl	Mixed-type/Langmuir isotherm	88.0%/50 ppm	WL, OCP, EIS, PDP, SEM, AFM, XPS, DFT and MD	The temperature was raised from 20 to 80 °C without affecting CHEC anticorrosion activity; at 80 °C, it demonstrated its best %IE of 93%.	65
Carboxymethyl cellulose (CMC)	Mild steel/2 M H_2SO_4	Langmuir isotherm	61%/0.5 g L^{-1} & 87%/0.5 g L^{-1} CMC + 5 mM KI.	WL.	At every temperature examined, the addition of Cl^- ions produced an antagonistic effect, but the addition of I^- ions produced a synergistic effect.	110

Table 1 (*continued*)

Nature of cellulose derivative	Nature of metal/electrolyte	Nature of inhibitor/ adsorption	Best %IE/optimum conc.	Techniques of study	Salient feature(s)	Ref.
Carboxymethyl cellulose (CMC)	Mild steel/2 M H_2SO_4	Mixed-type/Dubinin–Radushkevich isotherms	64.8%/0.5 g L^{-1}	WL and HE	%IE increases with the rise in conc and declines with the rise in temperature. CMC adsorption follows the physisorption mechanism.	113
Carboxymethyl cellulose (CMC)	Carbon steel/groundwater.	—	48%/250 ppm & 98% 250 ppm + 50 ppm Zn^{2+}.	WL, EIS and SEM.	There is a synergistic interaction between Zn^{2+} and CMC. SEM analysis validates the formation of a protective film, which is indicated by AC impedance spectra.	114
Carboxymethyl cellulose (CMC)	API 5 L X60 pipeline steel/CO_2 saturated 3.5% NaCl	Mixed-type/Langmuir isotherm	54.0%/100 ppm	PDP, EIS and SEM	EIS study suggests that at 60 °C, CMC is a better corrosion inhibitor (48%) than Ch (35%). However, the %IE of Ch and CMC is much less than that of the commercial inhibitor.	115
Carboxymethyl cellulose (CMC)	Carbon steel/1 M HCl and 1 M KOH	Mixed-type/Langmuir & Freundlich isotherms	79.7% (CMC;1 M HCl)/94.3 (1 M HCl; CMC + 0.5 PVP)/2.5 g L^{-1} CMC.	WL, PDP, DFT and MDS.	The inhibition efficiency of CMC was enhanced by adding additives, in that order: CMC + PAA < PVP + CMC < CMC + PVAc. In both mediums, the presence of CMC results in an increase in corrosion activation energy.	116
Sodium carboxymethyl cellulose (Na-CMC)	Copper/simulated water system	Mixed-type/Langmuir isotherm	79.32%/8 mg L^{-1}	EIS, PDP, AFM, FTIR and DFT.	Na-CMC used its carboxyl group to adsorb on the Cu surface. Adsorption energy was −60.823 kJ mol^{-1} on average.	117
Hydroxypropyl cellulose (HPC)	Aluminium/0.5 M HCl and 2 M H_2SO_4	Mixed-type/Langmuir isotherm	80.2% (HCl) and 65.3% (H_2SO_4)/5 g L^{-1}	WL, PDP and DFT.	Results demonstrated that concentration, time, temperature, metal-type, water content, and corrosion agent affect the %IE in HCl and H_2SO_4.	118
Sodium carboxymethyl cellulose (NaCMC)	Mild steel/1 M HCl	Mixed-type/Langmuir isotherm	54.1%/700 ppm & 86.77% (700 ppm + 1 ppm 16 × 10^{-16})	WL, EIS, PDP, FTIR, SEM and MD simulations.	An increase in the length of the surfactant tail causes a subsequent increase in the %IE.	119
Sodium carboxymethyl cellulose (NaCMC)	Aluminium/0.5 M HCl	Freundlich adsorption isotherm	86.58%/1 g L^{-1}	WL.	The rate at which corrosion occurs rises with an increase in operating temperature. After physisorption comes NaCMC adsorption.	120
Sodium carboxymethyl cellulose (NaCMC)	Mild steel/1 M HCl	Mixed-type/Langmuir isotherm	76.42%/2000 ppm; 85.85%/ 2000 + 500 KI & 88%/2000 + 500 KI.	WL and PDP.	NaCMC ability to inhibit growth was reduced with time and temperature increased. The %IE depended on temperature, immersion duration, compound concentration, and possibly their combined effect.	121
Methyl-cellulose (MC)	Magnesium/0.1 M HCl	Langmuir and Freundlich isotherms	71.45%/0.04 M	WL, HE, FT-IR and SEM.	The impact of $[H^+]$ on the degree of corrosion suggests that one of the degradation mechanisms of magnesium metal in the 0.1 HCl should include a step that determines the rate of H^+ presence.	122
Cellulose tetrazole (CTZ)	Carbon steel/1 M HCl	Cathodic-type/Langmuir isotherm	94.2%/100 ppm	WL, EIS, PDP, SEM, EDX, UV-vis, AFM and DFT.	Results show that the %IE rises with increasing CTZ conc and falls with increasing temperature. Double-layer capacitances also decrease in the blank solution.	51

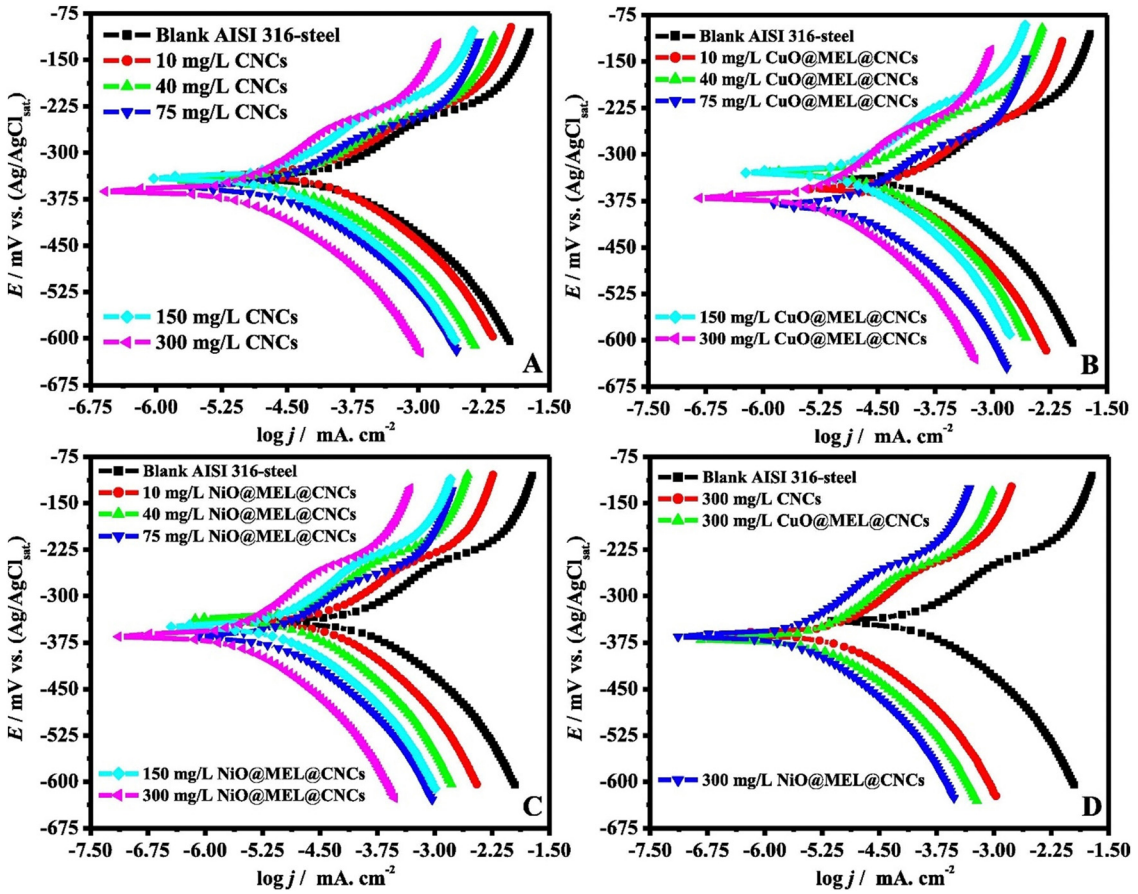

Fig. 11 PDP curves for AISI360-steel measured in 1.0 M H_2SO_4 solution with and without (blank) varying concentrations of (A) CNC, (B) CuO@MEL@CNCs and (C) NiO@MEL@CNCs, and (D) with 300 ppm of different nanocomposites present[133] [Reproduced from ref. 133 with permission; Copyright@Elsevier; 2021].

of the PANI/CMC composites, and a significant rise in inhibition efficiency (94.24% at 1000 ppm). The composites in corrosive solutions inhibit the anodic metal disintegration of the substrates and the cathodic H_2 reactions.

2.2.2. Nanocellulose and cellulose composites as anticorrosive coatings. For components working in highly corrosive environments, anti-corrosion coatings provide excellent protection against corrosion.[136,137] Three primary anti-corrosive coating alternatives can be distinguished: sacrificial, inhibitive, and barrier.[138] Barrier coatings cover a substrate to create a non-porous, protective layer that protects the base metal from environmental damage. It is considered unprotected if a barrier coating is applied to the base metal without any additional layer or film and the substrate is attacked by impact or chemicals. The film's solid content and thickness significantly impact the protection's longevity. A passive layer formed by inhibitory porous coatings on a substrate reacts with metal and humidity as it passes through the film. Inhibitory coatings are frequently used in overcoated primers because, over time, their ability to prevent corrosion diminishes dramatically. To protect the material underneath, sacrificial layers function as an additive over a substrate that corrodes sacrificially. In contrast to barrier coatings, sacrificial coatings keep working even if the film is damaged. However, the type of paint binder used and the amount of additive content affect the level of protection.

Recently, cellulose-based coatings have emerged as one of the most economical, efficient, and environmentally responsible methods.[73,139–143] The anticorrosive coatings made of cellulose have several benefits for a range of industrial uses. Cellulose-based coatings are more environmentally friendly because they are biodegradable and do not contribute to long-term environmental pollution. Unlike specific synthetic polymers dependent on petrochemicals, cellulose is primarily derived from renewable resources. Cellulose-based coatings are generally safer and non-toxic for application personnel and end users. Cellulose-based coatings decrease the risk of metal degradation because they have good adhesion and stop oxygen, humidity, and corrosive substances from penetrating. Because cellulose coatings can be adjusted and customized for particular uses, they are appropriate for various settings and businesses. Applying cellulose-based coatings with traditional coating methods like brushing, dipping, or spraying is frequently simple. Long-term corrosion protection requires a consistent and long-lasting protective layer, which cellulose-based coatings can help to create. It is simple to combine cellulose coatings with additional additives to improve

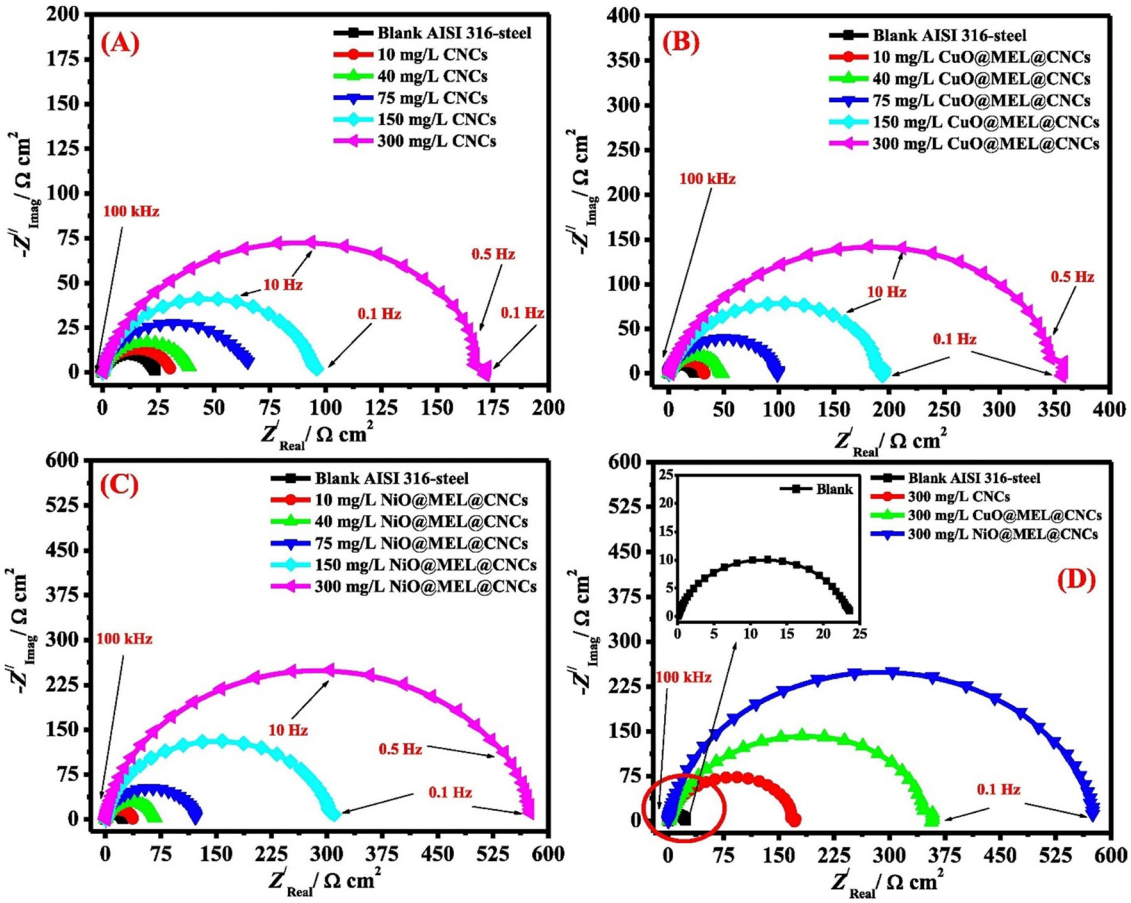

Fig. 12 Nyquist curves for AISI360-steel measured in 1.0 M H_2SO_4 solution with and without (blank) varying concentrations of (A) CNC, (B) CuO@MEL@CNCs and (C) NiO@MEL@CNCs, and (D) with 300 ppm of different nanocomposites present[133] [Reproduced from ref. 133 with permission; Copyright@Elsevier; 2021].

particular qualities like UV resistance, flexibility, or hardness. Often, cellulose is less expensive than some synthetic polymers.

A summary of some reports on cellulose-composites as anticorrosive coatings is presented in Table 2. Yabuki *et al.* showed that cellulose nanofibers improve the anticorrosion performance of the polymer coatings for the carbon steel/0.5%NaCl system.[144] Following a knife-edge scratch on the samples, polarization resistance was measured in NaCl solution and compared to a polymer coating that merely included a corrosion inhibitor; the scratched specimens combining nanofibers and the corrosion inhibitor had a higher polarization resistance. Following the corrosion test, voids on the coating of the polymer cross-section were verified, indicating that the nanofibers acted as channels for releasing the corrosion inhibitor. The coating comprised the right quantity of corrosion inhibitor (2%) and cellulose nanofibers (0.5%) for self-healing. Zhu and coworkers noticed that a cellulose-based coating (hydroxyapatite/aminated hydroxyethyl cellulose; (HA/AHEC)) improves the corrosion resistance and computability for AZ31 Mg alloy in simulated body fluid (SBF).[145] Polarization and EIS studies were conducted on bare AZ31 alloy coated with HA, AHEC, and HA/AHEC. The maximum decrease in current density and increase in charge transfer resistance or diameter of the Nyquist curve was observed in the presence of the HA/AHEC coating (Fig. 14). The anticorrosive applications of cellulose composites have also been explored in other studies.[72,146–149] Kreydie and. Al-Abdaly observed that metal oxides (ZnO:CuO and NiO:CuO) improve the anticorrosive activity of bacterial cellulose (BC).[146] The results demonstrated increased corrosion resistance by increasing coating concentrations of metallic nano-oxide.

Wu *et al.* studied mechanical and electrochemical capabilities based on modified cellulose nanofiber photoinitiators (MCNFI) and urushiol epoxy acrylate (UEA) and described their synthesis.[150] The synthesis of MCNFI/UEA is illustrated in Scheme 2. The outcomes demonstrated that the MCNFI/UEA coating features were better than those of the original UEA and the unaltered CNF (cellulose nanofiber) reinforced UEA (CFR/UEA) coating. The 8 wt% loading level produced the best mechanical properties; additional MCNFI loading decreased the mechanical properties. The structural features of the UEA matrix, which include suitable soft and hard segments and the fillers' good dispersibility and interfacial interaction, are responsible for the improved mechanical properties. The coating with MCNFI (8 wt%)/UEA showed the strongest anticorrosive properties. This study presented a novel technique

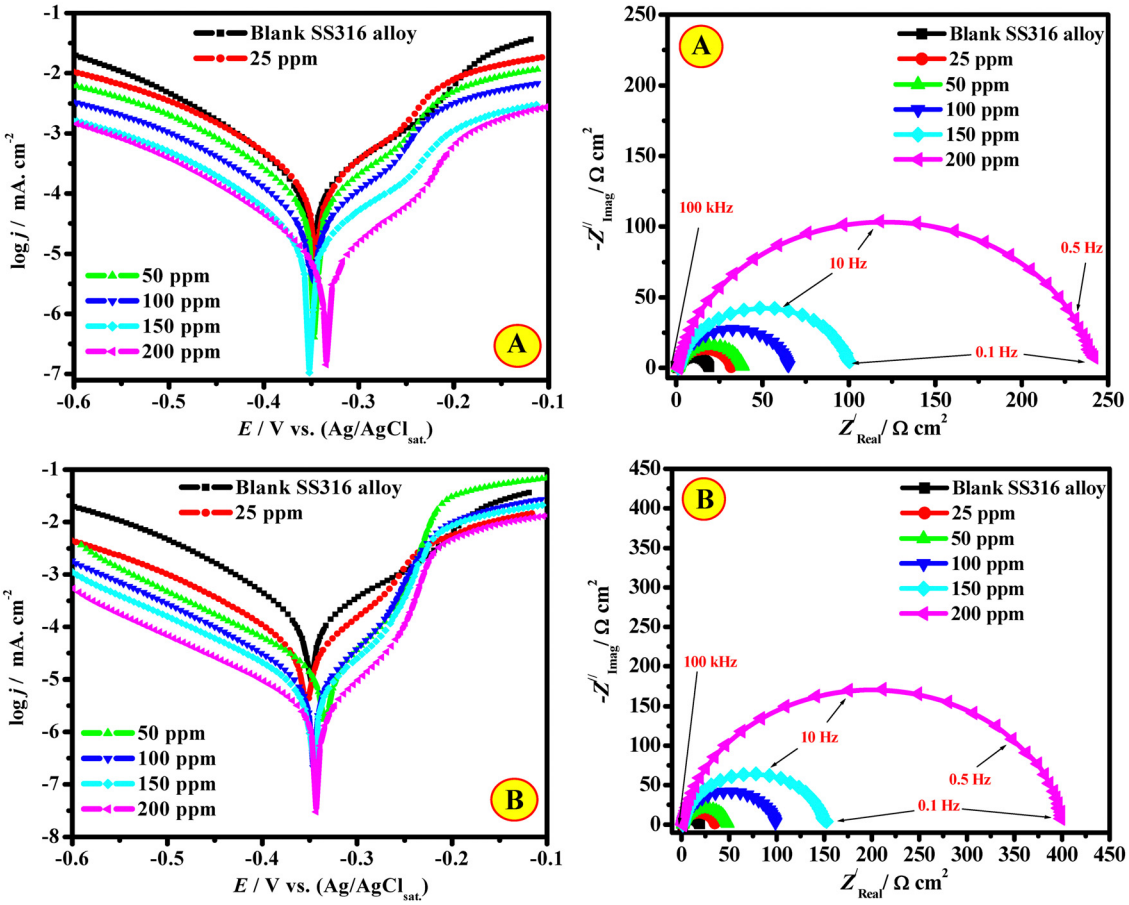

Fig. 13 PDP (left side) Nyquist (right side) diagrams of the SS316 alloy at T = 323 K in 2.0 M HCl with and without different concentrations of (A) CEL and (B) NCC[134] [Reproduced from ref. 134; open access publication, copyright permission not required].

for producing an anti-corrosive coating based on renewable urushiol that simultaneously uses modified nanocellulose as a filler and a macrophotoinitiator. The authors suggested that urushiol, UEA, had good low water absorption performance due to its long-side aliphatic chain. The composite coating's ability to decrease water absorption was guaranteed by the modified nanocellulose's hydrophobic properties when compared to the unmodified one.

The uniform distribution of CNFs in a polymer framework could be formed with grafting modification. The larger surface area and smaller size of CNFs make them an excellent nanofiller that increases the density of UEA coatings by allowing the coating to absorb more of the coating. Furthermore, the modified nanocellulose photoinitiator increased the coating's cross-link density by serving as an interface to connect the UEA molecule. It decreased its micropores, extending the corrosive medium's dissemination path through the coating and postponing the electrochemical corrosion process. Furthermore, since the coating included many oxygen atoms, the oxygen atom lone pair electrons could donate their charge to the Fe surface's d orbital. As a result, the coating may stick to the substrate and form a strong coordinate bond through chemisorption. The coating's hydroxyl groups may establish hydrogen bonds with the metal substrate to further improve adhesion. Corrosion was successfully postponed by the coating's strong adsorption force on the metal substrate. Finally, when O_2 increases close to the metal surface, an oxidation reaction occurs on the metal surface due to O_2 diffusion. Fe would be reduced to Fe^{3+} by oxidation, and Fe^{3+} would then react with the OH^- produced by the reduction reaction to form $Fe(OH)_3$ precipitation, covering the metal surface and creating a thick protective layer. To prevent corrosion from occurring again, the metal surface was passivated. The corrosion inhibition mechanism of the MCNFI/UEA composites is presented in Fig. 15.

Gouda and colleagues reported the formation of novel CeO_2-nanoparticle-loaded carboxymethyl cellulose (CeO_2–CMC), which was successfully made using an easy method and assessed using thermal, TEM, FT-IR, and FE-SEM/EDX analyses.[151] OCP, EIS, and PDP techniques examined the corrosion protection effectiveness of coated and unprotected mild steel with the CeO_2–CMC system in 1.0 M HCl solutions. MC simulation and DFT calculations also verified the connection between the coating film structure and corrosion protection. The produced CeO_2–CMC-coated coatings exhibited outstanding resistance to corrosion. The OCP assessment

Table 2 A summary of major reports on cellulose composites as anticorrosive coatings

Nature of coating material(s)	Nature of metal/electrolyte	Relative performance	Techniques of study	Salient feature(s)	Ref.
Microfibrillated cellulose nanofibers (CNFs) and calcium nitrite (CN).	Carbon steel/0.5%NaCl	Corrosion current density is reduced in the presence of CN.	PDP	The scrapped plain coating had a significantly greater anodic current density than the scratched CNF(0.5%) + CN(2%) and CN(4%) coatings. In contrast to the scratched CN(4%) coating, the anodized current density of the CNF(0.5%) + CN(2%) coating was significantly lower and the pitting potential was greater.	144
Hydroxyapatite/aminated hydroxyethyl cellulose (HA/AHEC) coating	AZ31 Mg alloy/simulated body fluid (SBF)	I_{corr} = AZ31 (2.23×10^{-6}); HA/AZ31 (3.93×10^{-6}); HEC/AZ31 (7.09×10^{-7}) and HA/AHEC/AZ31 (2.09×10^{-7}).	PDP, EIS and SEM.	The findings imply that the HA/AHEC composite-coated AZ31 magnesium alloy, with its good corrosion resistance and cytocompatibility, has potential use as a material for medical implants.	145
PU nanocrystalline cellulose composite (PNCCC) and PU micro-powdered cellulose composite (PMPCC)	Carbon steel/5%NaCl	96.68%; PU/MPC (1.0 wt%) and 96.92%; PU/NCC (1.0 wt%).	OCP, EIS, salt spray, and the mechanical properties measurements.	MPC and NCC positively impact the %IE of the polyurethane coatings. The best outcomes were acquired at a loading level of 1 wt%. MPC and NCC's embedding in the polyurethane coating improved the mechanical characteristics up to a loading level of 1.5 wt% and a higher level had a detrimental impact.	72
Bacterial cellulose/metal oxides nanocomposites [NBC/ZnO:CuO] & [NBC/NiO:CuO].	Carbon steel/3.5%NaCl	NBC/ZnO: CuO (97.31) and NBC/NiO:CuO % (93.37%).	PDP and OP	The findings showed that rising coating concentrations of metallic nano-oxide produced increased corrosion resistance.	146
Sodium oleate (S) adsorbed onto cellulose nanofibers (C) and zeolite particles (Z).	Carbon steel substrates/corrosive solution (different pH).	The existence of S significantly increased the degree of polarization resistance.	PR and SEM	The best mixtures for inhibiting corrosion were found to be 0.5 wt% zeolite particles with 0.4 wt% sodium oleate (S) and 1 wt% cellulose nanofibers with 8 wt% sodium oleate (C1-coating (S8 + Z0.5 − S0.4)).	147
Polyvinyl alcohol (EPVA) coating reinforced lignin nanocellulose (EPVA-LNC)	Q235 carbon steel/3.5%NaCl	$R_{ct} = 6.30 \times 10^2$ (Ω cm^2) (EPVA) and $R_{ct} = 1.99 \times 10^3$ (Ω cm^2)	FTIR, CA, OM, WAT and EIS.	The purpose of a heating treatment was to initiate elimination reactions among –OH groups. PVA's water absorption was drastically reduced, and its R_{ct} improved. The efficiency of a PVA composite coating reinforced by LNC was enhanced.	148
Nanocellulose in two pack epoxy polyamides (CNB).	Mild steel/3.5 wt% NaCl	$I_{corr} = 6.037 \times 10^{-4}$ (blank); 3.206×10^{-5} (STD), 8.779×10^{-7} (2% CNB), 4.8174×10^{-8} (4% CNB), 5.726×10^{-10} A cm^{-2} (6% CNB) for 120 h.	WL, EIS and PDP.	After being immersed for 120 hours at 6 wt% CNB, the impedance value can reach a maximum of 5×10^6. Studies on weight loss have also demonstrated that, after 120 hours, the corrosion rate is higher for 2, 4, and 6 wt% CNB when compared to bare and standard.	149
UV-curable nanocellulose/urushiol epoxy acrylate (UEA0) anticorrosive composite MCNFI/UEA.	Coating structure/3.5% NaCl	98.46%/MCNFI (8 wt%)/UEA	EIS, PDP, SEM, mechanical properties,	The MCNFI (8 wt%)/UEA sample showed the best resistance to corrosion. The mechanical properties and corrosion resistance of MCNFI/UEA first increased and then decreased with increasing MCNFI amount.	150
CeO_2-nanoparticle-loaded carboxymethyl cellulose (CeO_2–CMC)	Mild steel/1 M HCl	98.4%/3.0%CeO_2–CMC.	OCP, PDP, EIS, DFT and MCS.	The order of 3.0%CeO_2–CMC > 4.0%CeO_2–CMC > 5.0%CeO_2–CMC > 10.0%CeO_2–CMC > 2.0%CeO_2–CMC > 1.0%CeO_2–CMC was the protection abilities of the as-prepared CeO_2–CMC composites.	151
Epoxy resin-based nanocomposite (*ENT*) coatings	Mild steel/3.5% NaCl	96.21/*ENT* 2.0	PDP and EIS.	The ENT coatings were created and examined with different loadings of nanocellulose: 0.5 wt%, 1.0 wt%, 1.5 wt%, and 2.0 wt%. The outcomes showed that the sample with the best corrosion protection had 2.0 wt% nanocellulose derived from pineapple leaves.	152

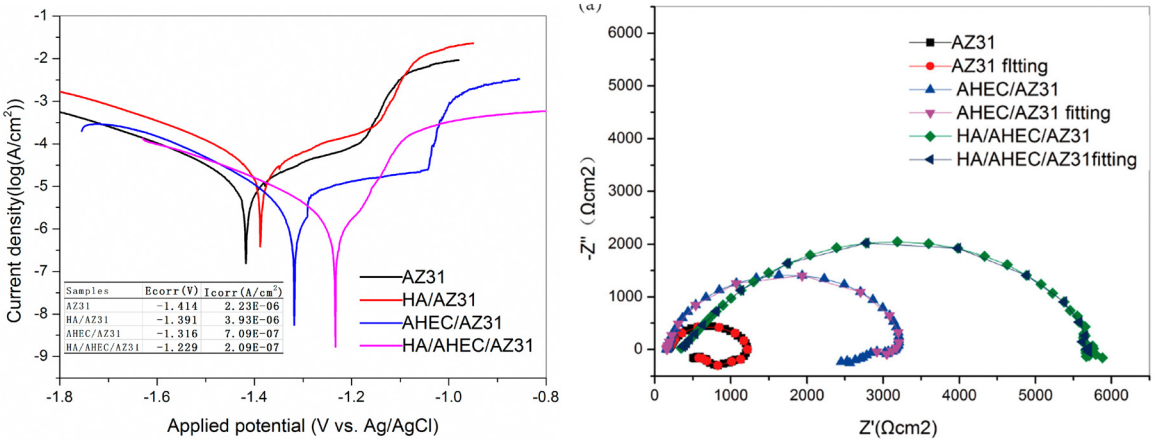

Fig. 14 The polarization (left side) and Nyquist (right side) plots for AZ31 corrosion in simulated body fluid with and without HA, AHEC and HA/AHEC coatings[145] [Reproduced from ref. 145; open access publication, copyright permission not required].

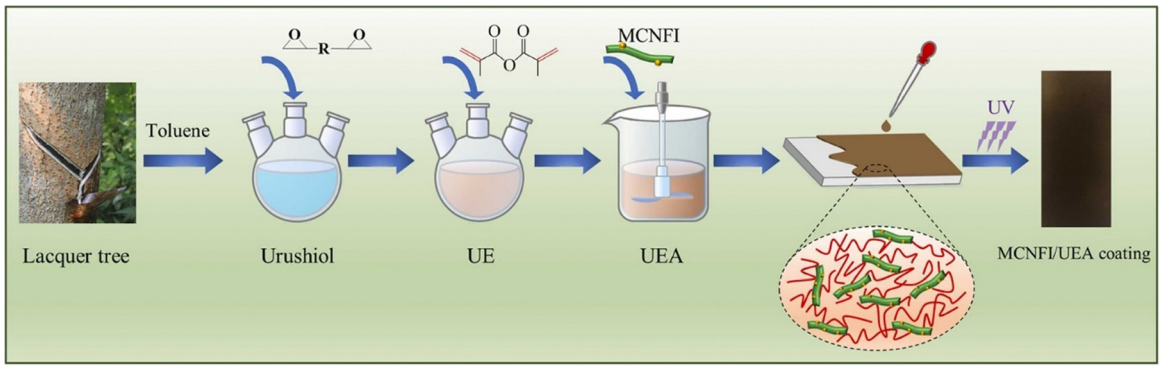

Scheme 2 Schematic presentation of the synthesis of MCNFI/UEA[150] [Reproduced from ref. 150 with permission; Copyright@Elsevier; 2022].

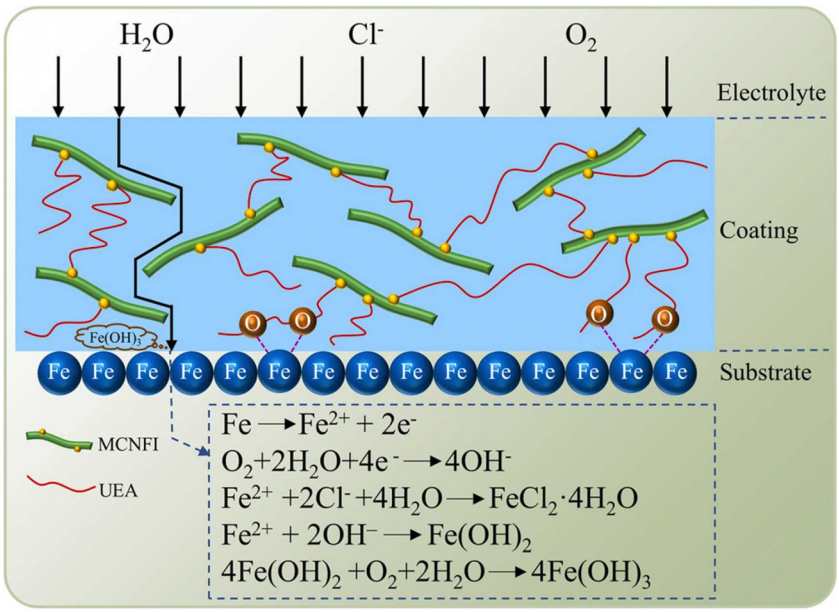

Fig. 15 Diagrammatic illustration of the MCNFI/UEA composite coatings' corrosion resistance mechanism on tinplate substrates[150] [Reproduced from ref. 150 with permission; Copyright@Elsevier; 2022].

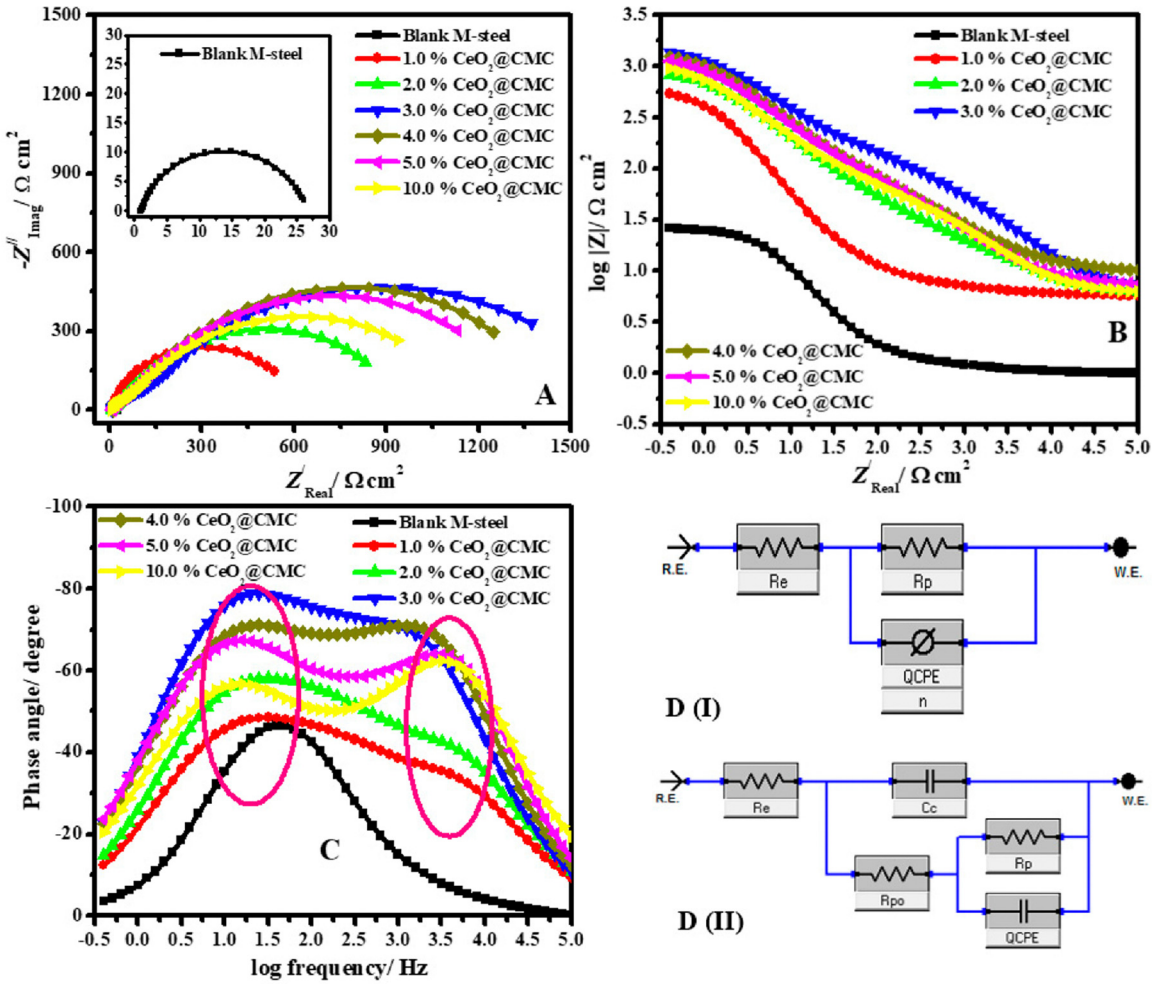

Fig. 16 Nyquist (A), Bode (B), and Bode phase (C) plots in 1.0 M HCl solution for MS and coated with different percentages of CeO_2–CMC at 50 °C, and (D) EEC for systems that are uncoated (D(I)) and coated (D(II))[151] [Reproduced from ref. 151; open access publication, copyright permission not required].

indicates that all the coated specimens exhibited additional positive potential during the initial immersion period compared to the blank MS. This suggests that the coated MS samples are in a passive state and are thus adequately shielded from acidic solutions. In a process that might be similar to anodic protection, the coated CeO_2–CMC films assisted in the formation of a persistent passive film. The EIS study was conducted for uncoated and coated MS surfaces to study the kinetic and interfacial properties of the coatings. The Nyquist and Bode phase angle and frequency plots are presented in Fig. 16.

In pure MS bare, the Nyquist diagram displays an individual capacitive loop, or solitary semicircle, attributed to the charge-transfer corrosion process. On the other hand, two capacitive loops are identified when coated MS surfaces with varying percentages of CeO_2–CMC nanocomposites are present. Based on information from research, the coating film capacitance (Q_{coat}, CPE_{coat}) and the coating film resistance (R_c) can be used to explain the inductive loop at relatively high-frequency (HF) areas. The polarization resistance (R_p) in conjunction with the double layer's capacitance (Q_{dl}, CPE_{dl}) may be responsible for the capacitive-loop regions at low frequencies (LF). The capacitive circles are slightly depressed and not quite perfect semicircles. This is connected to the frequency dispersion effect because of the imperfections and heterogeneity of the metal surface. The Bode impedance modulus exhibits linear regions at intermediate frequencies. The coated films exhibit even more linearity, suggesting steeper slopes than the uncoated metal. Recently, Grumo *et al.* demonstrated that the amount of nanocellulose (NC), used as a reinforced material in epoxy resin-based anticorrosive coatings, determines the overall corrosion inhibition effect.[152] The coating having the highest amount (2.0%) of NC showed the best efficiency of 96.21%.

3. Conclusion, research gaps, challenges and outlooks

The current discourse indicates that cellulose and its derivatives have exhibited encouraging potential as corrosion inhibitors in both the solution and coating phases. Because of its unique qualities, cellulose is a desirable option for corrosion

protection applications due to its renewable nature, biodegradability, and accessibility. Its solubility restricts the use of the aqueous phase in corrosion protection. However, cellulose derivatives, primarily carboxymethyl cellulose (CMC) and hydroxyethyl cellulose (HEC), are widely employed in corrosion prevention. They function as efficient inhibitors by adhering to the metal's surface and creating a barrier that shields it from corrosive attacks. By providing metal ions with binding sites, the hydroxyl groups in the cellulose molecules create a barrier that prevents corrosion on the metal surface. The concentration, temperature, and chemical composition of the solution are some variables that can affect the inhibition efficiency. The nature of the metal and electrolyte has a significant impact on the inhibition efficiency of cellulose. The results of the literature imply that appropriate synergists, such as halide ions (I^-, Br^-, *etc.*), metal cations (Zn^{2+}), surfactants (SDS, TX, CPC), and polymers (PVA, PAA, *etc.*), can be used to customize the %IE of cellulose derivatives. Nonetheless, the %IE of HEC is negatively impacted by chloride ions.

The %IE of cellulose derivatives in the solution phase can be shown using a variety of chemical, electrochemical, surface, and computational techniques, including WL, HE, OCP, EIS, PDP, FTIR, XRD, SEM, EDX, XPS, AFM, DFT, and MDS. To add another line of defence against corrosion during the coating phase, materials based on cellulose can be added to protective coatings. The cellulose-rich coating that forms prevents corrosive species from penetrating and encourages adhesion and cohesion, guaranteeing the metal substrate underneath long-term protection. They also become effective by offering an alternate path in the coating structures, which delays the penetration of the electrolytes. Although cellulose and its derivatives are promising as aqueous-phase corrosion inhibitors, several issues must be resolved before they can be used effectively. The solubility of cellulose and its derivatives in water may be restricted, which affects their capacity to form homogenous solutions. It can be challenging to achieve the ideal dispersion, so techniques to improve solubility must be investigated to guarantee even coverage on the metal surfaces. Since cellulose's protective films are typically weak and impacted by outside variables like pH, temperature, and exposure to harsh chemicals, their inhibitive qualities gradually deteriorate.

The processes used in synthesizing and modifying cellulose derivatives might not be environmentally friendly and could entail chemical treatments. Further research should investigate economical synthesis techniques and refine dosage specifications to render cellulose-derived inhibitors commercially feasible. Cellulose derivatives may only work well on some metal substrates. Thus, for cellulose-based inhibitors to be successfully applied in various industrial settings, research and development to understand the specificity of these inhibitors for different metals and alloys is essential. Fewer studies have been conducted on applying cellulose derivatives in the coating phase, which warrants further investigation. It is also necessary to investigate the corrosion inhibition mechanism during the coating phase, as it has yet to receive much attention in the literature. Research on the application of cellulose derivatives for the inhibition of corrosion in other metals and alloys, including aluminum, copper, zinc, and steel, is warranted as they are primarily utilized for protecting steel alloys (CS and MS) from corrosion.

Conflicts of interest

There are no conflicts to declare.

Acknowledgements

CV thankfully acknowledges the Khalifa University of Science and Technology for providing financial support under the postdoctoral fellowship.

References

1 D. Lavanya, P. Kulkarni, M. Dixit, P. K. Raavi and L. N. V. Krishna, *Int. J. Drug Formulation Res.*, 2011, **2**, 19–38.
2 A. A. Sundarraj and T. V. Ranganathan, *Drug Invent. Today*, 2018, **10**, 89–94.
3 H. A. Khalil, Y. Davoudpour, M. N. Islam, A. Mustapha, K. Sudesh, R. Dungani and M. Jawaid, *Carbohydr. Polym.*, 2014, **99**, 649–665.
4 E. S. Abd El-Sayed, M. El-Sakhawy and M. A.-M. El-Sakhawy, *Nord. Pulp Pap. Res. J.*, 2020, **35**, 215–230.
5 D. N.-S. Hon, *Chemical modification of lignocellulosic materials*, Routledge, 2017, pp. 97–127.
6 M. T. Postek, R. J. Moon, A. W. Rudie and M. A. Bilodeau, *Production and applications of cellulose*, Tappi Press, Peachtree Corners, 2013.
7 S. Ebnesajjad, *Handbook of adhesives and surface preparation*, Elsevier, 2011, pp. 137–183.
8 H. Mélida, J. V. Sandoval-Sierra, J. Diéguez-Uribeondo and V. Bulone, *Eukaryotic Cell*, 2013, **12**, 194–203.
9 W. Hu, S. Chen, J. Yang, Z. Li and H. Wang, *Carbohydr. Polym.*, 2014, **101**, 1043–1060.
10 A. K. Rana, E. Frollini and V. K. Thakur, *Int. J. Biol. Macromol.*, 2021, **182**, 1554–1581.
11 H. Seddiqi, E. Oliaei, H. Honarkar, J. Jin, L. C. Geonzon, R. G. Bacabac and J. Klein-Nulend, *Cellulose*, 2021, **28**, 1893–1931.
12 Y. Liu, S. Ahmed, D. E. Sameen, Y. Wang, R. Lu, J. Dai, S. Li and W. Qin, *Trends Food Sci. Technol.*, 2021, **112**, 532–546.
13 V. Varshney and S. Naithani, *Cellulose Fibers: Bio-and nano-polymer composites: Green chemistry and technology*, 2011, 43–60.
14 A. H. Saputra, L. Qadhayna and A. B. Pitaloka, *Int. J. Chem. Eng. Appl.*, 2014, **5**, 36.
15 T. Heinze, O. A. El Seoud and A. Koschella, *Cellulose derivatives: synthesis, structure, and properties*, Springer, 2018.

16 A. Blanco, M. C. Monte, C. Campano, A. Balea, N. Merayo and C. Negro, *Handbook of nanomaterials for industrial applications*, Elsevier, 2018, pp. 74–126.
17 B. L. Peng, N. Dhar, H. Liu and K. Tam, *Canadian J. Chem. Eng.*, 2011, **89**, 1191–1206.
18 P. Panchal, E. Ogunsona and T. Mekonnen, *Processes*, 2018, **7**, 10.
19 D. Klemm, K. Petzold-Welcke, F. Kramer, T. Richter, V. Raddatz, W. Fried, S. Nietzsche, T. Bellmann and D. Fischer, *Carbohydr. Polym.*, 2021, **254**, 117313.
20 B. Thomas, M. C. Raj, J. Joy, A. Moores, G. L. Drisko and C. Sanchez, *Chem. Rev.*, 2018, **118**, 11575–11625.
21 S. M. Rangappa, S. Siengchin, J. Parameswaranpillai, M. Jawaid and T. Ozbakkaloglu, *Polym. Compos.*, 2022, **43**, 645–691.
22 H. Sun, Y. Liu, X. Guo, K. Zeng, A. K. Mondal, J. Li, Y. Yao and L. Chen, *Chem. Eng. J.*, 2021, **425**, 131469.
23 S. Nie, N. Hao, K. Zhang, C. Xing and S. Wang, *Cellulose*, 2020, **27**, 4173–4187.
24 Z. Chen, Y. Hu, G. Shi, H. Zhuo, M. A. Ali, E. Jamróz, H. Zhang, L. Zhong and X. Peng, *Adv. Funct. Mater.*, 2023, 2214245.
25 L. Su, Y. Feng, K. Wei, X. Xu, R. Liu and G. Chen, *Chem. Rev.*, 2021, **121**, 10950–11029.
26 B. Moussian, *Targeting Chitin-Containing Organisms*, 2019, 5–18.
27 M. L. Verma, B. S. Dhanya, V. Rani, M. Thakur, J. Jeslin and R. Kushwaha, *Int. J. Biol. Macromol.*, 2020, **154**, 390–412.
28 Z. Wu, H. Li, X. Zhao, F. Ye and G. Zhao, *Carbohydr. Polym.*, 2022, **284**, 119182.
29 S. A. Umoren and U. M. Eduok, *Carbohydr. Polym.*, 2016, **140**, 314–341.
30 M. Shahini, B. Ramezanzadeh and H. E. Mohammadloo, *J. Mol. Liq.*, 2021, **325**, 115110.
31 C. Verma and M. Quraishi, *Int. J. Biol. Macromol.*, 2021, **184**, 118–134.
32 C. Verma and M. Quraishi, *Curr. Res. Green Sustainable Chem.*, 2021, **4**, 100184.
33 C. Verma, M. Quraishi, A. Alfantazi and K. Y. Rhee, *Int. J. Biol. Macromol.*, 2021, **184**, 135–143.
34 R. Ganjoo, S. Sharma, C. Verma, M. Quraishi and A. Kumar, *Int. J. Biol. Macromol.*, 2023, 123571.
35 C. Verma, E. E. Ebenso, M. Quraishi and C. M. Hussain, *Mater. Adv.*, 2021, **2**, 3806–3850.
36 W. Liu, K. Liu, H. Du, T. Zheng, N. Zhang, T. Xu, B. Pang, X. Zhang, C. Si and K. Zhang, *Nano-Micro Lett.*, 2022, **14**, 104.
37 S. Sulaiman, M. N. Mokhtar, M. N. Naim, A. S. Baharuddin and A. Sulaiman, *Appl. Biochem. Biotechnol.*, 2015, **175**, 1817–1842.
38 X. Guo, Y. Fu, F. Miao, Q. Yu, N. Liu and F. Zhang, *Ind. Crops Prod.*, 2020, **153**, 112575.
39 A. A. Ibrahim, A. M. Adel, Z. H. Abd El–Wahab and M. T. Al–Shemy, *Carbohydr. Polym.*, 2011, **83**, 94–115.
40 M. Gericke, J. Trygg and P. Fardim, *Chem. Rev.*, 2013, **113**, 4812–4836.
41 J. Qu, X. Tian, Z. Jiang, B. Cao, M. S. Akindolie, Q. Hu, C. Feng, Y. Feng, X. Meng and Y. Zhang, *J. Hazard. Mater.*, 2020, **387**, 121718.
42 S. Hokkanen, E. Repo, T. Suopajärvi, H. Liimatainen, J. Niinimaa and M. Sillanpää, *Cellulose*, 2014, **21**, 1471–1487.
43 E. Ituen, O. Akaranta and A. James, *Chem. Sci. Int. J.*, 2017, **18**, 1–34.
44 C. G. Vaszilcsin, M. V. Putz, A. Kellenberger and M. L. Dan, *J. Mol. Struct.*, 2023, **1286**, 135643.
45 R. Aslam, M. Mobin, S. Zehra and J. Aslam, *J. Mol. Liq.*, 2022, **364**, 119992.
46 L. Chen, D. Lu and Y. Zhang, *Materials*, 2022, **15**, 2023.
47 K. Y. Foo and B. H. Hameed, *Chem. Eng. J.*, 2010, **156**, 2–10.
48 X. Chen, M. F. Hossain, C. Duan, J. Lu, Y. F. Tsang, M. S. Islam and Y. Zhou, *Chemosphere*, 2022, **307**, 135545.
49 B. El Allaoui, H. Benzeid, N. Zari and R. Bouhfid, *J. Drug Delivery Sci. Technol.*, 2023, 104899.
50 C. Verma, M. A. Quraishi and K. Rhee, *Process Saf. Environ. Prot.*, 2022, **162**, 253–290.
51 S. A. Al Kiey, M. S. Hasanin and S. Dacrory, *J. Mol. Liq.*, 2021, **338**, 116604.
52 M. Gouda and H. M. A. El-Lateef, *Molecules*, 2021, **26**, 7006.
53 R. Randis, D. B. Darmadi, F. Gapsari, A. A. A. Sonief, E. D. Akpan and E. E. Ebenso, *J. Mol. Liq.*, 2023, 123067.
54 H. Wang, G. Gurau and R. D. Rogers, *Chem. Soc. Rev.*, 2012, **41**, 1519–1537.
55 K. N. Onwukamike, S. P. Grelier, E. Grau, H. Cramail and M. A. Meier, *ACS Sustainable Chem. Eng.*, 2018, **7**, 1826–1840.
56 A. Farrán, C. Cai, M. Sandoval, Y. Xu, J. Liu, M. J. Hernáiz and R. J. Linhardt, *Chem. Rev.*, 2015, **115**, 6811–6853.
57 M. E. Lamm, K. Li, J. Qian, L. Wang, N. Lavoine, R. Newman, D. J. Gardner, T. Li, L. Hu and A. J. Ragauskas, *Adv. Mater.*, 2021, **33**, 2005538.
58 Y.-Y. Li, B. Wang, M.-G. Ma and B. Wang, *Int. J. Polym. Sci.*, 2018, **2018**, 1–18.
59 M. P. Menon, R. Selvakumar and S. Ramakrishna, *RSC Adv.*, 2017, **7**, 42750–42773.
60 S. Vincent and B. Kandasubramanian, *Eur. Polym. J.*, 2021, **160**, 110789.
61 K. O. Reddy, C. U. Maheswari, M. Dhlamini, B. Mothudi, V. Kommula, J. Zhang, J. Zhang and A. V. Rajulu, *Carbohydr. Polym.*, 2018, **188**, 85–91.
62 A. Q. Almashhadani, C. P. Leh, S.-Y. Chan, C. Y. Lee and C. F. Goh, *Carbohydr. Polym.*, 2022, **286**, 119285.
63 J. Wang, L. Wang, D. J. Gardner, S. M. Shaler and Z. Cai, *Cellulose*, 2021, **28**, 4511–4543.
64 T. C. Mokhena and M. J. John, *Cellulose*, 2020, **27**, 1149–1194.
65 A. Farhadian, S. A. Kashani, A. Rahimi, E. E. Oguzie, A. A. Javidparvar, S. C. Nwanonenyi, S. Yousefzadeh and M. R. Nabid, *J. Mol. Liq.*, 2021, **338**, 116607.
66 U. Mamudu, M. R. Hussin, J. H. Santos and R. C. Lim, *Carbohydr. Polym. Technol. Appl.*, 2023, **5**, 100306.
67 G. Kumar, H. Kumar, R. Sharma, R. Kumari, A. Dhayal, A. Yadav and A. Yadav, *Next Mater.*, 2024, **2**, 100141.

68 J. Cui, Y. Bao, Y. Sun, H. Wang and L. Jing, *Composites, Part A*, 2023, 107729.
69 A. Kumar, B. Barik, P. G. Jablonski, S. Sonkaria and V. Khare, *Coatings*, 2022, **12**, 1674.
70 M. Baiardo, G. Frisoni, M. Scandola and A. Licciardello, *J. Appl. Polym. Sci.*, 2002, **83**, 38–45.
71 P. Stenstad, M. Andresen, B. S. Tanem and P. Stenius, *Cellulose*, 2008, **15**, 35–45.
72 M. Abd El-Fattah, A. M. Hasan, M. Keshawy, A. M. El Saeed and O. M. Aboelenien, *Carbohydr. Polym.*, 2018, **183**, 311–318.
73 A. Dastpak, P. Ansell, J. R. Searle, M. Lundstrom and B. P. Wilson, *ACS Appl. Mater. Interfaces*, 2021, **13**, 41034–41045.
74 A. Karimian, H. Parsian, M. Majidinia, M. Rahimi, S. M. Mir, H. S. Kafil, V. Shafiei-Irannejad, M. Kheyrollah, H. Ostadi and B. Yousefi, *Int. J. Biol. Macromol.*, 2019, **133**, 850–859.
75 T. Yi, H. Zhao, Q. Mo, D. Pan, Y. Liu, L. Huang, H. Xu, B. Hu and H. Song, *Materials*, 2020, **13**, 5062.
76 T. Kondo, *Polysaccharides*, 2005, 69–98.
77 A. Pinkert, K. N. Marsh and S. Pang, *Ind. Eng. Chem. Res.*, 2010, **49**, 11121–11130.
78 C. Verma, M. Quraishi and K. Rhee, *Adv. Colloid Interface Sci.*, 2022, **306**, 102723.
79 W. Liu, Z. Yan, X. Ma, T. Geng, H. Wu and Z. Li, *Materials*, 2018, **11**, 396.
80 X. Qiu and S. Hu, *Materials*, 2013, **6**, 738–781.
81 T. Gan, Y. Zhang, M. Yang, H. Hu, Z. Huang, Z. Feng, D. Chen, C. Chen and J. Liang, *Ind. Eng. Chem. Res.*, 2018, **57**, 10786–10797.
82 E. E. Ebenso, C. Verma, L. O. Olasunkanmi, E. D. Akpan, D. K. Verma, H. Lgaz, L. Guo, S. Kaya and M. A. Quraishi, *Phys. Chem. Chem. Phys.*, 2021, **23**, 19987–20027.
83 C. Verma, M. Quraishi and K. Y. Rhee, *Chem. Eng. J.*, 2022, **430**, 132645.
84 X. Zhou, Y. Wang, C. Gong, B. Liu and G. Wei, *Chem. Eng. J.*, 2020, **402**, 126189.
85 F. Rol, M. N. Belgacem, A. Gandini and J. Bras, *Prog. Polym. Sci.*, 2019, **88**, 241–264.
86 M. Yadav, G. Goel, F. L. Hatton, M. Bhagat, S. K. Mehta, R. K. Mishra and N. Bhojak, *Curr. Res. Green Sustainable Chem.*, 2021, **4**, 100153.
87 Y. Lvov and E. Abdullayev, *Prog. Polym. Sci.*, 2013, **38**, 1690–1719.
88 Z. Xu, Y. Zhao, J. Wang and H. Chang, *Appl. Therm. Eng.*, 2019, **148**, 1074–1080.
89 D. Rahmadiawan, Z. Fuadi, R. Kurniawan, H. Abral, F. Ilhamsyah, A. Arafat, B. Syahri and E. Indrawan, *Tribol. Industry*, 2022, **44**, 584.
90 C. Nwoye, K. Amanze, N. Okelekwe, M. Joseph and C. Ibe.
91 S.-C. Shi and C.-C. Su, *Materials*, 2016, **9**, 612.
92 N. A. Al-Rubaiey and F. S. Kadhim, *Al-Khwarizmi Eng. J.*, 2019, **15**, 125–133.
93 Z. Xu, Y. Zhao, Y. Yan and H. Zhang, *Comput. Mater. Sci.*, 2023, **228**, 112295.
94 I. Arukalam, I. Madufor, O. Ogbobe and E. Oguzie, *Chem. Eng. Commun.*, 2015, **202**, 112–122.
95 I. Okechi Arukalam, I. Chimezie Madufor, O. Ogbobe and E. E. Oguzie, *Pigm. Resin Technol.*, 2014, **43**, 151–158.
96 E. Bayol, A. Gürten, M. Dursun and K. Kayakirilmaz, *Acta Phys.-Chim. Sin.*, 2008, **24**, 2236–2243.
97 M. R. Sovizi and R. Abbasi, *J. Adhes. Sci. Technol.*, 2020, **34**, 1664–1678.
98 G. Sedahmed, M. N. Soliman and N. El-Kholy, *J. Appl. Electrochem.*, 1982, **12**, 479–485.
99 I. O. Arukalam, *Acad. Res. Int.*, 2012, **2**, 35–42.
100 M. N. El-Haddad, *Carbohydr. Polym.*, 2014, **112**, 595–602.
101 Y. Sangeetha, S. Meenakshi and C. S. Sundaram, *Carbohydr. Polym.*, 2016, **150**, 13–20.
102 V. Rajeswari, D. Kesavan, M. Gopiraman and P. Viswanathamurthi, *Carbohydr. Polym.*, 2013, **95**, 288–294.
103 I. Arukalam, I. Madufor, O. Ogbobe and E. Oguzie, *The Open Corrosion J.*, 2014, **6**, 1–10.
104 I. Arukalam, I. Madufor, O. Ogbobe and E. Oguzie, *British J. Appl. Sci. Technol.*, 2014, **4**, 1445.
105 I. Arukalam, I. Madufo, O. Ogbobe and E. Oguzie, *Int. J. Appl. Sci. Eng. Res.*, 2014, **3**, 241–256.
106 I. Arukalam, I. Madu, N. Ijomah, C. Ewulonu and G. Onyeagoro, *J. Mater.*, 2014, **2014**, 1–11.
107 I. Arukalam, *Carbohydr. Polym.*, 2014, **112**, 291–299.
108 M. Deyab, *J. Power Sources*, 2015, **280**, 190–194.
109 M. Mobin and M. Rizvi, *Carbohydr. Polym.*, 2017, **156**, 202–214.
110 S. Umoren, M. Solomon, I. Udosoro and A. Udoh, *Cellulose*, 2010, **17**, 635–648.
111 M. Sobhi and S. Eid, *Prot. Met. Phys. Chem. Surf.*, 2018, **54**, 893–898.
112 P. Boonsa and A. Rodchanarowan, *Mater. Res. Express*, 2020, **7**, 066519.
113 M. Solomon, S. Umoren, I. Udosoro and A. Udoh, *Corros. Sci.*, 2010, **52**, 1317–1325.
114 N. Manimaran, S. Rajendran, M. Manivannan, J. A. Thangakani and A. S. Prabha, *Eur. Chem. Bull.*, 2013, **2**, 494–498.
115 S. A. Umoren, A. A. AlAhmary, Z. M. Gasem and M. M. Solomon, *Int. J. Biol. Macromol.*, 2018, **117**, 1017–1028.
116 S. Nwanonenyi, H. Obasi and A. Chidiebere, *J. Bio- Tribo-Corrosion*, 2018, **4**, 1–12.
117 M.-M. Li, Q.-J. Xu, J. Han, H. Yun and Y. Min, *Int. J. Electrochem. Sci.*, 2015, **10**, 9028–9041.
118 S. Nwanonenyi, H. Obasi and I. Eze, *Chemistry Africa*, 2019, **2**, 471–482.
119 R. Aslam, M. Mobin, J. Aslam, H. Lgaz and I.-M. Chung, *J. Mater. Res. Technol.*, 2019, **8**, 4521–4533.
120 O. Egbuhuzor, I. Madufor, S. Nwanonenyi and J. Bokolo, *Nigerian J. Technol.*, 2020, **39**, 369–378.
121 U. Itodoh, I. Madufor, M. Obidiegwu and E. Oguzie, *Moroccan J. Chem.*, 2023, **11**(11–12), 2521–2540.
122 R. M. Hassan and S. M. Ibrahim, *J. Mol. Struct.*, 2021, **1246**, 131180.
123 H. Shaghaleh, X. Xu and S. Wang, *RSC Adv.*, 2018, **8**, 825–842.

124 B. G. Janesko, *Phys. Chem. Chem. Phys.*, 2011, **13**, 11393–11401.
125 G. Singh, G. Singh and T. S. Kang, *Phys. Chem. Chem. Phys.*, 2018, **20**, 18528–18538.
126 A. Kafy, K. K. Sadasivuni, H.-C. Kim, A. Akther and J. Kim, *Phys. Chem. Chem. Phys.*, 2015, **17**, 5923–5931.
127 R. Reshmy, E. Philip, S. A. Paul, A. Madhavan, R. Sindhu, P. Binod, A. Pandey and R. Sirohi, *Rev. Environ. Sci. Bio/Technol.*, 2020, **19**, 779–806.
128 I. Oladele, L. Onuh, G. Ogunwande and S. Borisade, *Green Hybrid Composite in Engineering and Non-Engineering Applications*, Springer, 2023, pp. 113–136.
129 B. Aaliya, K. V. Sunooj and M. Lackner, *Int. J. Biobased Plast.*, 2021, **3**, 40–84.
130 M. M. Solomon, H. Gerengi and S. A. Umoren, *ACS Appl. Mater. Interfaces*, 2017, **9**, 6376–6389.
131 M. S. Hasanin and S. A. Al Kiey, *Int. J. Biol. Macromol.*, 2020, **161**, 345–354.
132 H. M. A. El-Lateef, W. Albokheet and M. Gouda, *Cellulose*, 2020, **27**, 8039–8057.
133 H. M. Abd El-Lateef and M. Gouda, *J. Mol. Liq.*, 2021, **342**, 116960.
134 A. Toghan, M. Gouda, K. Shalabi and H. M. A. El-Lateef, *Polymers*, 2021, **13**, 2275.
135 Y. Lu, H. Feng, H. Xia and W. H. Xia, *Int. J. Electrochem. Sci.*, 2022, **17**, 221180.
136 D. Thomas, E. Philip, R. Sindhu, S. B. Ulaeto, A. Pugazhendhi and M. K. Awasthi, *Biomass Convers. Biorefin.*, 2022, **12**, 4683–4699.
137 S. He, Y. Gao, X. Gong, C. Wu and H. Cen, *J. Coat. Technol. Res.*, 2023, **20**, 819–841.
138 A. Popoola, O. Olorunniwo and O. Ige, *Dev. Corros. Prot.*, 2014, **13**, 241–270.
139 F. Calegari, B. C. da Silva, J. Tedim, M. G. Ferreira, M. A. Berton and C. E. Marino, *Prog. Org. Coat.*, 2020, **138**, 105329.
140 C. Borsoi, L. C. Scienza, A. J. Zattera and C. A. Ferreira, *Mater. Res.*, 2018, **21**, 1–10.
141 F. Calegari, I. Sousa, M. G. Ferreira, M. A. Berton, C. E. Marino and J. Tedim, *Appl. Sci.*, 2022, **12**, 1800.
142 B. Anyanwu, O. Oluwole, O. Fayomi, A. Olorunnisola, A. Popoola and S. Kuye, *Case Stud. Chem. Environ. Eng.*, 2021, **3**, 100017.
143 K. S. M. Ubas, J. C. Grumo, A. G. Ruda, M. T. Bonilla, A. A. B. Mutia, J. P. Labis, N. L. B. Sayson and A. C. Alguno, *Solid State Phenom.*, 2023, **351**, 103–115.
144 A. Yabuki, A. Kawashima and I. W. Fathona, *Corros. Sci.*, 2014, **85**, 141–146.
145 B. Zhu, Y. Xu, J. Sun, L. Yang, C. Guo, J. Liang and B. Cao, *Metals*, 2017, **7**, 214.
146 S. Kreydie and B. Al-Abdaly, *Euras. Chem. Commun.*, 2021, **3**, 706–714.
147 A. Yabuki, M. Kanagaki, C. Nishikawa, J. H. Lee and I. W. Fathona, *Prog. Org. Coat.*, 2021, **154**, 106194.
148 J. Zhang, Y. Huang, H. Wu, S. Geng and F. Wang, *Prog. Org. Coat.*, 2021, **155**, 106224.
149 S. Devadasu, S. H. Sonawane and S. Suranani, *Mater. Today: Proc.*, 2021, **46**, 5544–5549.
150 H. Wu, X. Han, W. Zhao, Q. Zhang, A. Zhao and J. Xia, *Ind. Crops Prod.*, 2022, **181**, 114805.
151 M. Gouda, M. M. Khalaf, M. A. Al-Shuaibi, I. M. Mohamed, K. Shalabi, R. M. El-Shishtawy and H. M. A. El-Lateef, *Polymers*, 2022, **14**, 3078.
152 J. Grumo, A. Lubguban, R. Capangpangan, A. Yabuki and A. Alguno, *Mater. Today: Proc.*, 2023, **37**, 107478.

